

Phase Equilibrium Modeling of Structure H Clathrate Hydrates of Methane + Water “Insoluble” Hydrocarbon Promoter Using QSPR Molecular Approach

Ali Eslamimanesh,[†] Farhad Gharagheizi,[‡] Amir H. Mohammadi,^{*,†,§} and Dominique Richon[†]

[†]MINES ParisTech, CEP/TEP - Centre Énergétique et Procédés, 35 Rue Saint Honoré, 77305 Fontainebleau, France

[‡]Saman Energy Giti Co., Postal Code: 3331619636, Tehran, Iran

[§]Thermodynamics Research Unit, School of Chemical Engineering, University of KwaZulu-Natal, Howard College Campus, King George V Avenue, Durban 4041, South Africa

 Supporting Information

ABSTRACT: In this communication, the quantitative structure–property relationship (QSPR) strategy is applied to present two molecular models for determination of the structure H (sH) hydrate dissociation conditions with methane as help gas. Twenty-one water “insoluble” hydrocarbon promoters are examined. To propose reliable models, almost all of the available literature data are studied. Two mathematical methods including the genetic-algorithm-based multivariate linear regression (GA-MLR) and the least square support vector machines (LSSVM) are applied for determination (selection) of the model parameters. As a result, two reliable models are developed: (1) QSPR-GA-MLR linear model and (2) QSPR-LSSVM nonlinear model with satisfactory results quantified by the following statistical parameters: absolute average deviations (AAD) of the represented/predicted hydrate dissociation pressures from existing experimental values: about 9%, and squared correlation coefficient: 0.956 in the case of using the first model, and about 4% and 0.992 through applying the second model, respectively. These results demonstrate much better accuracy through the QSPR-LSSVM nonlinear model than applying the QSPR-MLR linear one.

1. INTRODUCTION

Gas hydrates (or clathrate hydrates) are crystalline solid compounds composed of water and small molecules like CO₂, N₂, methane (CH₄), hydrogen (H₂), etc. under suitable conditions of low temperatures and high pressures.^{1–7} They are a subset of compounds known as clathrates (originating from the Greek word “khlatron”) or inclusion compounds.^{1,7} A clathrate compound is one, in which a molecule or molecules of one/several components (guest molecules) is/are enclosed in a structure built from molecules of another component (host molecules).^{1,7} The majority of gas hydrates are known to form three typical hydrate crystal structures: structure I (sI), structure II (sII), and structure H (sH).^{1–7} The type of crystal structure generally depends on the size of the guest molecule(s).^{1,7}

Formation of gas hydrates was found to be one of the reasons for blockage of transportation pipelines in the natural gas industry in early 1930s.^{1,7,8} Therefore, this phenomenon results in a reduction of the pipelines cross sectional area and consequently excess pressure drop during transportation of natural gases, leading to high production/processing/transportation costs and low production/processing/transportation rates, and also fouling in pipelines leading to restricted flow.^{1,7,8} In contrast to the mentioned disadvantages, there are many positive applications of clathrate hydrates, e.g. in CO₂ capture and sequestration, gas storage, air-conditioning systems in the form of hydrate slurry, water desalination/treatment technology, concentration of dilute aqueous solutions, separation of different gases from flue gas streams, etc., which have been reported, especially in recent years.^{1–4,9}

Several studies show that the gas hydrate structures have considerable potential for storage of various gases. For instance, they can be used for natural gas/hydrogen storage and transportation,^{10–37} as cool storage media in air conditioning systems, etc.^{38–41} Storage and transportation in the form of gas hydrates have the advantages of safety of the corresponding processes, much lower required space, and lower production costs compared with conventional storage methods like liquefaction.^{10–37} It has been demonstrated that it is not suitable to use liquefied natural gas or pipeline transportation for a medium or small scale natural gas field, where the natural gas hydrate formation process is a more economical approach.¹⁰

However, slow gas hydrate formation rates and high pressure/low temperature conditions for industrial applications of clathrate hydrate storage processes are among the factors that have been subjects of many studies recently. Gas hydrate promoters have been generally considered as additives to the hydrate crystallization (formation) processes to greatly reduce the required hydrate formation pressure and increase the formation rate and/or temperature along with modification of the selectivity of hydrate cages for absorption of various gas molecules in the water cages or increase in the storage capacity of these structures.^{42–74}

The common gas hydrate formation promoters can be categorized into two distinct groups: (1) water “soluble” and (2) water “insoluble”. The first group can consist of mainly

Received: May 6, 2011

Accepted: July 13, 2011

Published: September 13, 2011

two branches of substances including those that do not take part in the structures of the hydrate cages, e.g., tetrahydrofuran (THF), 1,4-dioxane, 1,3-dioxalane, acetone, etc.,^{42–47} which normally form structure II of clathrate hydrates in the presence/absence of gas molecules^{42–47} and the ones that take part in the structures of the hydrate cages such as tetra-*n*-butylammonium halides (TBAX) especially tetra-*n*-butylammonium bromide (TBAB) and other halides like tetrabutyl phosphonium bromide (TBPB),^{48–74} which form semiclathrate hydrates. THF from the first and TBAB from the latter categories are the well-known water-soluble thermodynamic promoters that have been well-investigated in the past decade.^{42–74}

The thermodynamic models presented in the literature dealing with the representation/prediction of the clathrate hydrate phase equilibria of the systems containing water-soluble organic promoters (first category) are generally based on the equality of fugacities/chemical potentials of the components in the phases present.^{47,75–79} The van der Waals–Platteeuw⁸⁰ (vdW-P) model is applied for evaluation of the fugacity/chemical potential of water in the hydrate phase. For instance, Kamran-Pirzaman et al.⁸¹ and Illbeigi et al.⁸² have recently proposed a thermodynamic model to calculate/estimate the phase equilibria of corresponding systems containing THF applying the UNIFAC group contribution model to evaluate the activity coefficient of water and THF in the aqueous phase. They obtained acceptable results in comparison with the literature data. Another approach for this purpose has been reported by Mohammadi and co-workers,^{83,84} who successfully studied the use of the well-known artificial neural networks (ANNs) mathematical tool. However, very few models have been presented in the literature regarding the phase behaviors of semiclathrate hydrates (second category). Mohammadi et al.,⁸⁵ investigated the application of ANNs for acceptable representation/prediction of the semiclathrate hydrate of hydrogen dissociation conditions for the systems including TBAB aqueous solutions before the stoichiometric ratio. Recently, Paricaud⁸⁶ proposed a thermodynamic model based on the use of the statistical associating fluid theory with variable range for electrolytes (SAFT-VRE)⁸⁷ dealing with aqueous phase and vdW-P⁸⁰ for solid (hydrate) phase. He reported acceptable agreement between the predicted dissociation temperatures of the system of hydrates formed in the carbon dioxide + TBAB aqueous solution and corresponding experimental data. New scientific projects are currently in progress to present simpler models and also generate required experimental phase equilibrium data for this issue.⁸⁸ All of the aforementioned models have been developed for special systems and they still require extension to all water-soluble hydrate formers.

Water “insoluble” promoters could be some heavy hydrocarbons like cyclopentane, cyclohexane, methyl cyclohexane, etc.,^{1,18,82} which normally form structure H (cyclopentane and cyclohexane form structure II).^{1,18,82} Structure H hydrate formers occupy the large cages of hydrate structure and may be used to increase gas storage capacity of clathrate hydrates.

Several experimental studies have been made to determine the effect of water insoluble hydrate formers on hydrate dissociation conditions of various gases especially methane.^{18,89–96} For instance, it has been shown that the presence of methyl cyclohexane can considerably increase the hydrate dissociation temperature or decrease the hydrate dissociation pressure of the methane + water system.⁸⁹ However, methyl cyclohexane does not have strong promotion effects on the hydrogen sulfide + water system.⁸⁹ Similar effects have been previously reported regarding the cyclopentane/

cyclohexane + hydrogen sulfide + water system, though the promotion effect of cyclopentane or cyclohexane is considerable compared with the methyl cyclohexane promoter.^{90,91}

Very limited experimental data for the systems containing heavy hydrocarbon promoters + ethane/carbon dioxide/nitrogen are available.^{92,93} It was argued that the ethane molecule may competitively occupy the large cages of sII hydrate with cyclopentane or cyclohexane and may consequently occupy large cages competitively with methyl cyclohexane in sH clathrate hydrate.⁹³ Experimental measurements show that the promotion effects of heavy hydrocarbon promoters on the systems containing carbon dioxide clathrate hydrates are not as considerable as the effects on the methane clathrate hydrates. However, these effects on the nitrogen clathrate hydrates are high but may not be of great interest in gas storage processes as natural gases generally do not contain high amounts of nitrogen.^{92,93} Moreover, experimental studies have proven that benzene can shift the hydrate dissociation conditions of the methane + water system, but toluene and dimethylbenzenes have almost little or no effect on the dissociation conditions of methane hydrates.⁹⁶

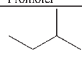
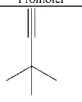

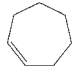
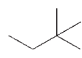

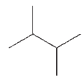
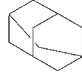
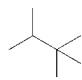
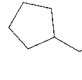
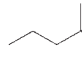
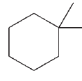
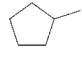
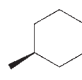
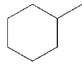
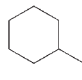
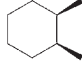
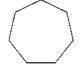
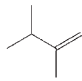
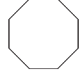
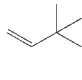
The theoretical efforts to model the phase equilibria of the aforementioned water “insoluble” hydrate formers are almost similar to those ones performed on the systems containing water-soluble promoters. For instance, the thermodynamic models are generally based on equality of fugacities of the components throughout all present phases. However, the presence of the fourth phase may lead to divergence of the flash calculations algorithms in these kinds of models because they are literally dependent on the initial guess for the initial amounts of the fourth phase, e.g., liquid hydrate former-rich phase. Furthermore, the corresponding solubility data in water required to tune the especially adopted thermodynamic models are limited. This fact indicates another limitation of the related algorithms. Another point is that most of the reported thermodynamic models have been checked for especial kinds of promoters and their capabilities to account for the effects of other heavy hydrocarbon hydrate formers on gas hydrate dissociation conditions have not been examined yet. On the other hand, applications of the traditional numerical methods like ANNs may be conservative for this purpose because the physical properties such as critical pressure, temperature, and acentric factors, which can be used to identify the kind of hydrate promoter, may not guaranty to acceptably train these networks for representation/prediction of dissociation conditions of sH clathrate hydrates.

Therefore, there is still a need to develop accurate, predictive and reliable models for this purpose. In this study, we propose novel approaches based on the quantitative structure–property relationship (QSPR) strategy to determine the dissociation conditions of structure H clathrate hydrates in the systems containing water “insoluble” hydrocarbon promoter + methane + water. This is the first time that this kind of molecular model is applied to gas hydrate modeling.

2. EXPERIMENTAL DATA AND MATHEMATICAL METHODS

2.1. Experimental Database. Accuracy and reliability of the models generally depends on the validity/comprehensiveness of the employed data set for their development.^{97–128} In this work, we tried to apply most of the available experimental data regarding the structure H hydrate dissociation conditions for the water “insoluble” hydrocarbon promoter + methane + water

Table 1. Chemical Structures of the Studied Water “Insoluble” Hydrocarbon Promoters along with Other Information

ID	Promoter	Name	CAS Number	Formula	ID	Promoter	Name	CAS Number	Formula
1		2-methylbutane	78-78-4	C ₅ H ₁₂	12		3,3-Dimethyl-1-butyne	917-92-0	C ₆ H ₁₀
2		2,2-dimethylpropane	463-82-1	C ₅ H ₁₂	13		Cycloheptene	628-92-2	C ₇ H ₁₂
3		2,2-dimethylbutane	75-83-2	C ₆ H ₁₄	14		cis-Cyclooctene	931-87-3	C ₈ H ₁₄
4		2,3-Dimethylbutane	79-29-8	C ₆ H ₁₄	15		Adamantane	281-23-2	C ₁₀ H ₁₆
5		2,2,3-Trimethylbutane	464-06-2	C ₇ H ₁₆	16		Ethylcyclopentane	1640-89-7	C ₇ H ₁₄
6		2,2-Dimethylpentane	590-35-2	C ₇ H ₁₆	17		1,1-Dimethylcyclohexane	590-66-9	C ₈ H ₁₆
7		Methylcyclopentane	96-37-7	C ₆ H ₁₂	18		cis-1,4-Dimethylcyclohexane	624-29-3	C ₈ H ₁₆
8		Methylcyclohexane	108-87-2	C ₇ H ₁₄	19		Ethylcyclohexane	1678-91-7	C ₈ H ₁₆
9		cis-1,2-Dimethylcyclohexane	2207-01-4	C ₈ H ₁₆	20		Cycloheptane	291-64-5	C ₇ H ₁₄
10		2,3-Dimethyl-1-butene	563-78-0	C ₆ H ₁₂	21		Cyclooctane	292-64-8	C ₈ H ₁₆
11		3,3-Dimethyl-1-butene	558-37-2	C ₆ H ₁₂					

systems.^{129–145} The chemical structures and other information about the investigated clathrate hydrate promoters (21 promoters) are reported in Table 1.

2.2. Determination of Molecular Descriptors. Molecular descriptors are defined as numerical characteristics associated with chemical structures.^{98,103,116–128,146–148} They are basic molecular properties of a compound and normally determined from the chemical structure. Each type of molecular descriptors is related to a specific type of interactions between chemical groups in a particular molecule.^{98,103,116–128,146–148} Several software packages are generally used for the computation of molecular descriptors of a large number of chemical structures. A review of these software packages can be found in the work of Todeschini and Consonni.¹⁴⁶ In this study, one of the most widely used software packages, “Dragon”,¹⁴⁷ has been employed. This software is able to calculate more than 3000 molecular descriptors for any desired chemical structure. So far, these molecular descriptors have been determined for about 234 000 pure compounds using Dragon software, which is freely available¹⁴⁸ (many of these compounds have not been synthesized up to now). Since the values of many descriptors are related to the bond lengths, bond angles, etc., each chemical structure is generally optimized before

calculation of its molecular descriptors. For this purpose, chemical structures of all 21 promoters have been sketched in Hyperchem software¹⁴⁹ and optimized using the MM+ (the classical molecular dynamics) molecular mechanics force field. Finally, the molecular descriptors have been determined using the Dragon software.¹⁴⁷

2.3. Developing the Models. Having calculated the molecular descriptors from the optimized chemical structures of all investigated promoters, a linear equation is presented, which is able to represent/predict the desired parameter (hydrate dissociation pressure) with the smallest number of variables as well as the highest accuracy.^{98,103,116–128,146–148} In other words, the objective is to find a subset of variables (most statistically effective molecular descriptors on the dissociation conditions) from all available variables (all molecular descriptors) that are able to represent/predict the hydrate dissociation pressure with the lowest possible deviation from the experimental values. A generally accepted method for this purpose is using the genetic algorithm-based multivariate linear regression (GA-MLR).^{150,151} In this method, the genetic algorithm is applied to select the best subset of variables based on an objective function, as first performed by Leardi et al.¹⁵² in 1992. Fitness functions such as

R^2 , adjusted R^2 , Q^2 , “Akaike” information content (measure of the goodness of fit of an estimated statistical model), etc. are normally applied as objective functions in GA-MLR technique.^{150,151} The “RQK” fitness function is a novel one proposed to avoid undesired model properties such as chance correlation, presence of noisy variables in the models, and other model pathologies causing lack of model prediction capability.¹⁵⁰ Moreover, RQK is a constrained fitness function based on Q^2_{LOO} statistics (leave-one-out cross validated variance) and other four tests that must be fulfilled contemporarily. The detailed description of this function is presented in the Supporting Information.

In this study, the RQK function is used as the fitness function. The results of application of GA-MLR with RQK fitness function have been satisfactory in the previous works.^{98,103,116–128,146–148} In order to use the GA-MLR algorithm, a computer program has been written in MATLAB environment.

The main data set is generally divided into two subdata sets before pursuing the GA-MLR^{150,151} computational steps including the “Training” set and the “Test (prediction)” set. In this paper, these sets are defined as follows: the “Training” set is used to generate the model and the “Test” set is used to test the prediction capability of the obtained model. The process of division of the main data set into two subdata sets is performed randomly. For this purpose, about 80% and 20% of the main data set are randomly selected for the “Training” set (about 238 data), and the “Test” set (about 60 data). The effect of the allocation percent of the two subdata sets from the data of main data set on the accuracy of the model has been already discussed.¹⁵⁵

Several validation techniques are generally used to obtain a valid and reliable model. In this work, the methods recommended by Todeschini et al.¹⁵³ including the bootstrapping, y-scrambling, and external validation techniques have been applied, well-established in the Supporting Information.

Having selected the most proper molecular descriptors, and consequently derived a linear correlation between these descriptors and hydrate dissociation pressure of the investigated systems, they have been further treated as the input variables of a mathematical algorithm for developing the nonlinear QSPR model, i.e., the nonlinear relations between the desired output and the selected molecular descriptors. For this purpose, we have investigated the use of the least-squares support vector machine (LSSVM) strategy.¹⁵⁵

Although ANN models have been generally proven to provide high accuracy for different problems,^{83,84,97–102,156} they have the disadvantages of random initialization of the networks and variation of the stopping criteria during optimization of the model parameters.^{156–159} The support vector machine (SVM) is a well-known strategy developed from the machine-learning community.^{156–159} The advantages of the SVM methods over the traditional ANNs are as follows:^{156–161}

1. More probability for convergence to the global optimum;
2. Normally find a solution that can be quickly obtained by a standard algorithm (quadratic programming);
3. Need not to determine the network topology in advance; which can be automatically determined as the training process ends;
4. There may be generally less probability of the SVM strategy to be faced with overfitting problem.

The SVM outstanding performance makes it perhaps superior to the traditional empirical risk minimization principles. Furthermore, as a result of their specific formulation, sparse solutions can

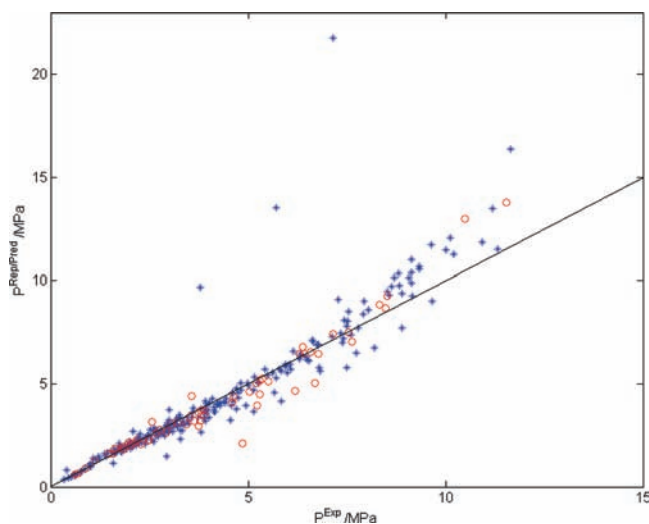


Figure 1. Comparison between the represented (Rep)/predicted (Pred) results of the first developed GA-MLR¹⁵⁰ linear model (eq 1) and experimental values^{129–145} of hydrate dissociation conditions of the investigated systems. P , pressure (MPa). *, Training set; O, test (prediction) set. The straight curve represents the unity of squared correlation coefficient.

be found and both linear and nonlinear regressions can be performed.^{156,158,161}

Suykens and Vandewalle¹⁶¹ have reported a modification to the original SVM to overcome the difficulty of the previous algorithm in finding the final solution because it requires the solution of a set of nonlinear equations (quadratic programming). Their method, named as least-squares SVM (LSSVM),¹⁶¹ encompasses the advantages similar to those of SVM though it requires solving a set of only linear equations (linear programming), which is much easier and more rapid compared to the traditional SVM method.^{156,158,161}

In the LSSVM¹⁶¹ approach, the regression error is defined as the difference between the represented/predicted property values and experimental ones, which is considered as an addition to the constraints of the optimization problem. In traditional SVM method, the value of the regression error is generally optimized during the calculations while in the LSSVM,¹⁶¹ the error is mathematically defined.^{156,158,161} The detailed descriptions of the LSSVM¹⁶¹ equations and computational steps of the applied algorithm are presented as Supporting Information.

3. RESULTS AND DISCUSSION

Application of several mathematical strategies was investigated in order to obtain the best linear model. For this purpose, the selected molecular descriptors and their quadratic values were considered as the inputs of the model. In addition, several function transforms of the hydrate dissociation pressure (P) were treated as the output parameters such as $\log(P)$, $\log(P + 1)$, $(P + 0.5)^2$, $P^{-0.5}$, $1/P$, and $1/(P + 1)$.¹⁵² These function transforms are the most-widely used ones, which have been normally used in QSPR methods to model the nearly linear problems.¹⁵² As a result, $P^{-0.5}$ transform was founded to contribute to the more accurate results than the others. Therefore, an accurate linear equation between $P^{-0.5}$ and the pool of molecular descriptors was obtained using the GA-MLR¹⁵⁰ computational procedure. For obtaining this equation, the best linear two-molecular descriptor model was

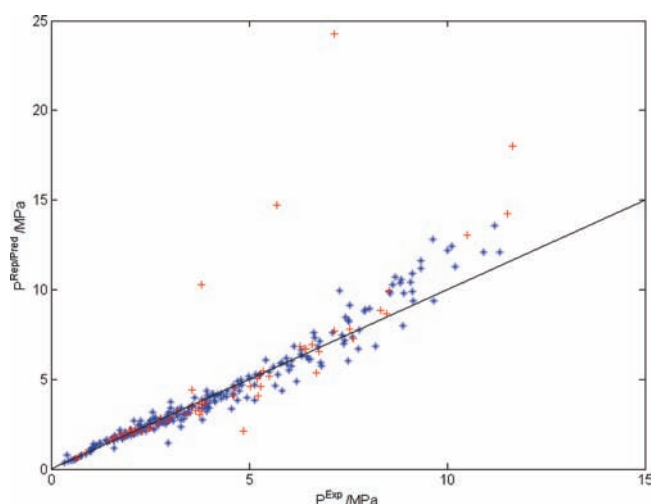


Figure 2. Comparison between the represented (Rep)/predicted (Pred) results of the second developed GA-MLR¹⁵⁰ linear model (eq 1) and experimental values^{129–145} of hydrate dissociation conditions of the investigated systems. P , pressure (MPa). *, Training set; +, test (prediction) set. The straight curve represents the unity of squared correlation coefficient.

determined.^{98,103,116–128,146–148} This procedure was repeated to develop the most accurate three, four, five, etc. molecular descriptors linear models.

Figure 1 depicts the represented/predicted hydrate dissociation conditions applying the primary obtained model vs experimental data.^{129–145} However, it can be observed from these results that four of the represented values have much higher deviations from experimental values^{129–145} than the other ones. In order to further investigate the reliability of these four experimental values, we developed another linear model, considering them in the test (prediction) set instead of the training set. Figure 2 shows the subsequent deviations of the hydrate dissociation pressure values, calculated/estimated by the second linear model. It is inferred that the corresponding deviations for these four points have been again much higher than the rest of the points and also their relative deviations in comparison with the other represented/predicted points are almost the same as determined by the first model. Therefore, we may conclude that these four data points are erroneous or at least they can be regarded as the outliers of the developed linear model. As a consequence, a new (third) linear model has been developed applying all of the experimental data^{129–145} except those four points. It was demonstrated that the most accurate GA-MLR¹⁵⁰ linear model contains five parameters because further increase in the number of molecular descriptors does not lead to any considerable effects on the accuracy of the obtained model. The final equation is presented as follows:

$$\begin{aligned}
 P^{-1/2} = & -0.6164[E]_{ij} (\pm 0.00508) - 0.19452Mor12v (\pm 0.02823) \\
 & + 0.70527E1u (\pm 0.07074) \\
 & + 0.15301HATS4u^2 (\pm 0.00499) \\
 & - 0.00006T^2 + 4.06466 (\pm 0.06332) \quad (1)
 \end{aligned}$$

The numbers of digits of the reported coefficient values of eq 1 are generally in agreement with the results of conventional computer algorithms using GA-MLR¹⁵⁰ models. In eq 1

- “ E ” is the seventh eigenvalue from “edge adjacency” matrix weighted by dipole moment. The “edge adjacency matrix”

or the “bond matrix” is derived from the molecular graph denoted information about the connectivity of the graph edges. It is a square symmetric matrix of dimension $B \times B$, where B is the number of bonds and is generally derived from the Hydrogen-depleted molecular graph. It is defined as¹⁴⁶

$$[E]_{ij} = \begin{cases} 1 & \text{if } (i, j) \text{ are adjacent bonds} \\ 0 & \text{otherwise} \end{cases} \quad (2)$$

The “edge adjacency matrix”, weighted by dipole moment, is defined based on the “edge adjacency matrix”, in which the diagonal elements are the dipole moments of the corresponding bond. It is somehow a measure of the polarity of the molecule;

- “ $Mor12v$ ” is a “3D-MORSE descriptor” (3D-molecule representation of structures based on electron diffraction), which is weighted by “van der Waals volume”. It is defined as¹⁴⁶

$$Mor12v = \sum_{i=1}^{n_{AT}-1} \sum_{j=i+1}^{n_{AT}} v_i v_j \frac{\sin(12r_{ij})}{12r_{ij}} \quad (3)$$

where n_{AT} , v , and r_{ij} are the total number of atoms, van der Waals volume of a specific atom, and the distance between the i th and j th atoms in a molecule. It is a measure of molecular size and shape.

- “ $E1u$ ” is a directional “WHIM” descriptor. It is the result of performing “principal component analysis” on the centered “Cartesian” coordinates of a molecule. The covariance between the j th and k th coordinates is defined as follows:¹⁴⁶

$$s_{jk} = \sum_{i=1}^{n_{AT}} (q_{ij} - \bar{q}_j)(q_{ik} - \bar{q}_k) \quad (4)$$

where q_{ij} and q_{ik} represent the j th and k th coordinates (j and $k = x, y, z$) of i th atom, respectively, and \bar{q} is the corresponding average value. “ $E1u$ ” is calculated as follows:¹⁴⁶

$$E1u = \frac{\lambda_1^2 n_{AT}}{\sum t_{j1}^2} \quad (5)$$

where λ_1 is the first eigenvalue of the covariance matrix of the atomic coordinates, which refers to atomic coordinates with respect to the k axes, and t_{j1} is the value of the members of a definite row of the covariance matrix. It is a measure of molecular size.

- “ $HATS4u$ ” is a “GATAWAY” descriptor. It is defined as¹⁴⁶

$$HATS4u = \sum_{i=1}^{n_{AT}} \sum_{j \geq i}^{n_{AT}} h_i h_j \delta(d_{ij}; 1) \quad (6)$$

where $\delta(d_{ij}; 1)$ is “Dirac delta” function, which is equal to 1 when the topological distance between atoms i and j is equal to 1, and it is equal to 0, otherwise. “ h_i ” is the leverage of the i th atom. These leverages are diagonal elements of the molecular influence matrix (\mathbf{H}) which is defined as¹⁴⁶

$$\mathbf{H} = \mathbf{M} \times (\mathbf{M}^T \times \mathbf{M})^{-1} \times \mathbf{M}^T \quad (7)$$

where \mathbf{M} is the molecular matrix formed by the centered “Cartesian” coordinates x, y, z of the molecule atoms (including hydrogen) in a chosen conformation. Atomic coordinates are

assumed to be calculated with respect to the geometrical center of the molecule to obtain translational invariance. The molecular influence matrix is a symmetric $n_{AT} \times n_{AT}$ matrix.

The traditional statistical parameters of the developed linear model are as follows

$$n_{\text{training}} = 235, \quad n_{\text{test}} = 59, \quad R_{\text{training}}^2 = 0.9720, \\ R_{\text{test}}^2 = 0.9331, \quad \text{RMS} = 0.042, \quad F = 1587.1$$

where n_{training} and n_{test} are the numbers of experimental hydrate dissociation data treated in training set and test set, respectively, R_{training}^2 and R_{test}^2 are the squared correlation coefficients of the training set and test set results, respectively, RMS is the root mean squared error of the representations/predictions of the model compared with the experimental values,^{129–145} and F is the F -ratio of the obtained GA-MLR¹⁵⁰ linear equation (eq 1), which is defined as the ratio between the model summation of squares (MSS) and the residual summation of squares (RSS):^{156,162}

$$F = \frac{\text{MSS}/df_M}{\text{RSS}/df_E} \quad (8)$$

where df_M and df_E refer to the degrees of freedom of the model and the overall error, respectively. It is a comparison between the model explained variance and the residual variance. It should be noted that high values of the F -ratio tests indicate high reliability of the developed models.

For internal validation of the model, leave-one-out cross validation technique was initially used. The corresponding parameter is normally calculated as follows:^{98,103,116–128,146–148,156}

$$Q_{\text{Loo}}^2 = 1 - \frac{\sum_{i=1}^n (y_i - \hat{y}_{ic})^2}{\sum_{i=1}^n (y_i - \bar{y})^2} \quad (9)$$

where y_i is the hydrate dissociation pressure for i th system, \bar{y} is mean value of hydrate dissociation pressure for all of the investigated systems, and \hat{y}_{ic} is response of i th object represented/predicted by the obtained model ignoring the value of the related object (i th experimental hydrate dissociation pressure). The smallest absolute difference between this value and the R^2 parameter shows the highest reliability of the model. The evaluated leave-one-out cross validation parameter of the obtained linear model is 0.9650.

Another statistical parameter for internal validation of the QSPR linear model is the adjusted- R^2 parameter, which is defined as follows:^{98,103,116–128,146–148,156}

$$R_{\text{adj}}^2 = 1 - (1 - R^2) \left(\frac{n-1}{n-p'} \right) \quad (10)$$

where n is the number of experimental values and p' is the number of model parameters. The smallest absolute difference between this value and the R^2 parameter indicates the highest reliability of the model. The evaluated adjusted- R^2 parameter of the obtained linear model is 0.9713.

As mentioned earlier, for testing the validity of the first developed model, we have used several validation techniques including, bootstrap technique, y -scrambling, and external validation techniques, which are explained in detail in the Supporting Information file.^{98,103,116–128,146–148,156} Consequently, the value of Q_{boot}^2 parameter (bootstrap parameter) of the obtained model

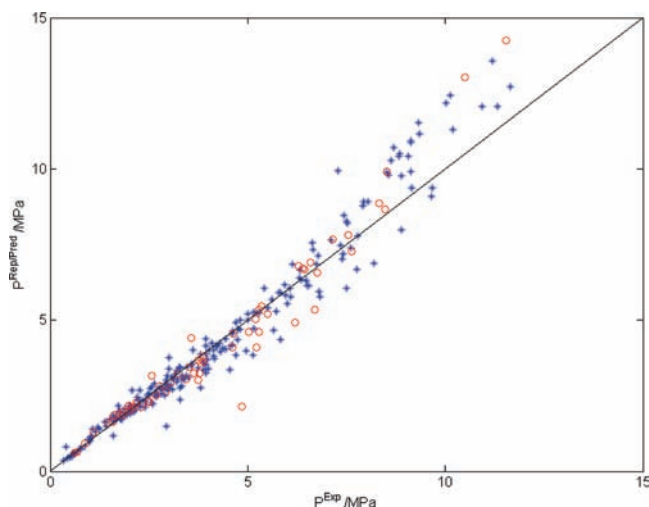


Figure 3. Comparison between the represented (Rep)/predicted (Pred) results of the final (third) developed GA-MLR¹⁵⁰ linear model (eq 1) and experimental values^{129–145} of hydrate dissociation conditions of the investigated systems. P , pressure (MPa). *, Training set; O, test (prediction) set. The straight curve represents the unity of squared correlation coefficient.

was evaluated to be 0.9629, the value of intercept a (y -scrambling parameter) was calculated as -0.015 for the developed linear model, and the evaluated Q_{ext}^2 (external validation parameter) of the obtained linear model was determined to be 0.973.

Figure 3 depicts the represented/predicted hydrate dissociation conditions by eq 1 versus experimental data.^{129–145} The deviations of these results in comparison with the experimental values^{129–145} have been better interpreted in Figure 4. All of the calculated/estimated hydrate dissociation pressure values by eq 1, and the corresponding deviations from experimental values,^{129–145} accompanied with the detailed allocation of the molecular descriptors in each organic promoter are extensively presented as Supporting Information.

The selected molecular descriptors were later treated using the LSSVM¹⁶¹ mathematical method to develop a more accurate and reliable model. The selected molecular descriptors by the GA-MLR^{150,151} model were considered as the input parameters of the LSSVM¹⁶¹ strategy. The two main parameters of this algorithm are σ^2 and γ , which are supposed to be optimized using a proper optimization method. However, selecting the best optimization procedure for this purpose is still a challenge. To select the most efficient optimization method, the following characteristics of the corresponding algorithm should be taken into account:^{156,164–172}

1. Ability to handle nondifferentiable, nonlinear, and multimodal cost functions;
2. No requirement of extensive problem formulation. In traditional methods (such as integer programming, geometric programming, branch and bound methods, etc.) special mathematical formulation is necessary to determine a problem;
3. Ease of use, i.e., few control variables to steer the minimization. These variables should also be robust and easy to choose;
4. No sensitivity to starting point;
5. Good convergence properties, i.e., consistent convergence to the global optimum in consecutive independent trials.

Due to the preceding characteristics and the high nonlinearity of the SVM algorithm, application of nonpopulation based

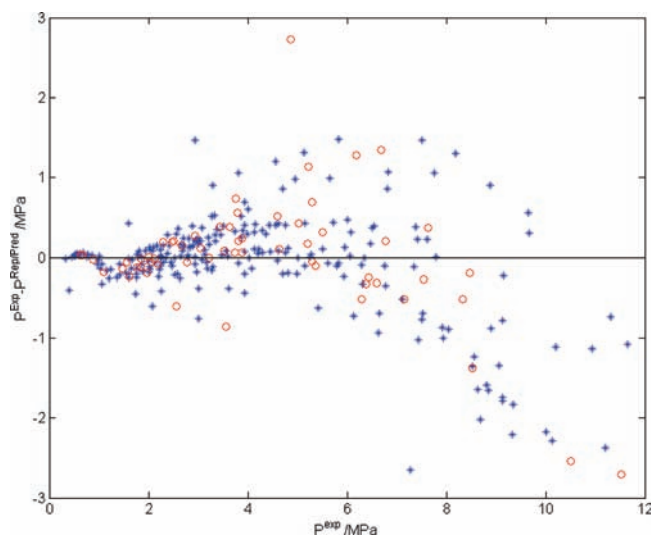


Figure 4. Deviations of the determined hydrate dissociation pressure values of the studied systems by eq 1 from experimental values.^{129–145} P , pressure (MPa). *, Training set; O, test (prediction) set. The straight curve represents the unity of squared correlation coefficient.

optimization methods such as simplex simulated annealing algorithm (M-SIMPASA),¹⁷³ and Levenberg–Marquardt (LM)¹⁷⁴ may be conservative.¹⁵⁶

In this work, we have modified the optimization part of the LSSVM¹⁶¹ algorithm developed by Pelckmans et al.¹⁶² and Suykens and Vandewalle¹⁶¹ to use the robust hybrid genetic algorithm (H-GA) method.^{167,168} This modification not only results in quicker computational steps but also leads the optimization procedure to be insensitive to the starting points. For this purpose, the traditional genetic algorithm¹⁵¹ has been hybridized with pattern-search method to perform the local optimization more accurate and faster than the traditional genetic algorithm method.¹⁵¹ Therefore, the optimization toolbox of MATLAB software has been implemented, which is able to perform parallel computations. This feature may effectively decrease the required time of the optimization process to converge to the global optimum. The number of populations of the optimization algorithm applied in this work was set to 1000. In order to ensure that the value of the final solution was very close to the global optimum of the problem, the optimization procedure was repeated for several times. In the next step, the database is divided into three subdata sets including the “Training” set, the “Validation (Optimization)” set, and the “Test” set. In this study, the “Training” set is used to generate the model structure, the “Validation (Optimization)” set is applied for optimization of the model, and the “Test (prediction)” set is used to investigate the prediction capability and validity of the proposed model. The division of the database into three subdata sets is normally performed randomly. For this purpose, about 80%, 10%, and 10% of the main data set are randomly selected for the “Training” set (206 data points), the “Optimization” set (44 data points), and the “Test” set (44 data points).

Results of a particular computational route to achieve the optimum parameters of the LSSVM¹⁶¹ model are shown in Figure 5. The value of the probable global optimum of the problem (although determination of the real global optimum of the problem may not be generally easy); that is, a compromise between all of the local optima can be well-interpreted in the

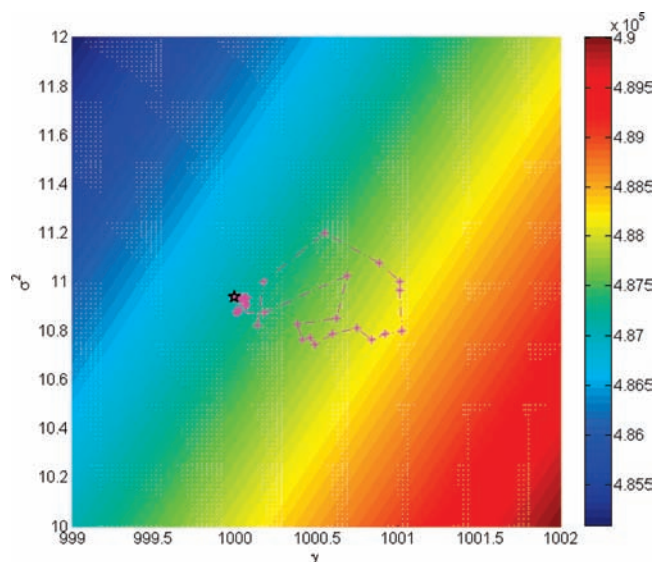


Figure 5. Contour route of the H-GA^{167,168} optimization algorithm in LSSVM¹⁶¹ mathematical approach: * along with dashed line, the computational route to converge to the global optimum of the problem; ☆, the probable global optimum of the problem. σ^2 and γ are the parameters of the LSSVM¹⁶¹ model.

figure. A large difference between the values of the LSSVM¹⁶¹ parameters leads to us not being able to show all of the local optima of the problem during the optimization procedure. However, it is possible to observe these values by scaling-up the presented figure. The optimized values of the parameters of the LSSVM¹⁶¹ algorithm were calculated as follows: $\gamma = 1000$ and $\sigma^2 = 10.935$. The numbers of the reported digits of the two aforementioned parameters are normally obtained by sensitivity analysis of the overall errors of the optimization procedure to the corresponding values.

The determined hydrate dissociation conditions and their deviations using the developed QSPR-LSSVM model vs the experimental values,^{129–145} are reported in Figures 6 and 7, respectively. Moreover, the statistical parameters of this model are shown in Table 2. All of the determined pressure values by the developed QSPR-LSSVM nonlinear model, the corresponding deviations from experimental values,^{129–145} and the detailed allocation of the molecular descriptors in each organic promoters are extensively presented as Supporting Information. The *mat* files (MATLAB file format) of the obtained model (developed as software) is also presented as Supporting Information file and the instructions for running the developed computer program is well indicated in the Appendix. Therefore, anyone can easily apply the software (by running the program) to reproduce all of our results and predict phase equilibria of the investigated systems at temperature conditions of interest. All of the required parameters as inputs of the computer program for any kind of heavy hydrocarbon hydrate formers (studied in this work) can be easily observed in the Supporting Information XLS file.

Careful investigation of the Figures and Table 3 shows that the absolute deviations of the calculated/estimated hydrate dissociation conditions from experimental values^{129–145} do not pursue similar trends by increasing the experimental values regarding the two developed models (QSPR-GA-MLR and QSPR-LSSVM). Furthermore, the corresponding absolute relative deviations for a particular hydrate dissociation pressure may be so different applying each of the developed models. This is mainly due to the

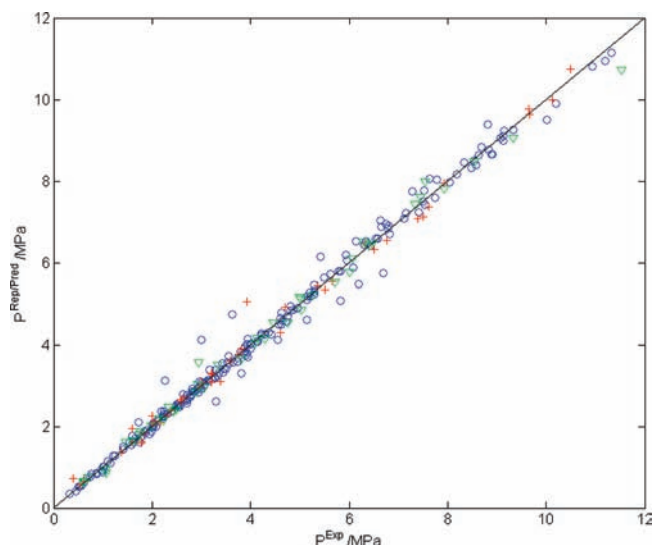


Figure 6. Comparison between the represented (Rep)/predicted (Pred) results of the developed QSPR-LSSVM model and experimental values^{129–145} of hydrate dissociation conditions of the investigated systems. P , pressure (MPa). \circ , Training set; +, validation (optimization) set; Δ , test (prediction) set. The straight curve represents the unity of squared correlation coefficient.

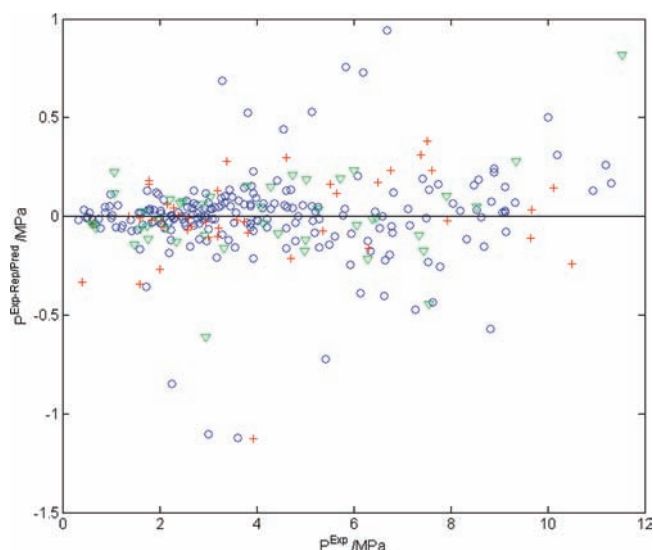


Figure 7. Deviations of the determined hydrate dissociation pressure values of the studied systems by the QSPR-LSSVM model from experimental values.^{129–145} P , pressure (MPa). \circ , Training set; +, validation (optimization) set; Δ , test (prediction) set. The straight curve represents the unity of squared correlation coefficient.

following factors: 1. The different mathematical basis of these models. For instance, the GA-MLR^{150,151} linear model leads the absolute deviations to increase linearly in comparison with the experimental values^{129–145} because this model has been developed based on solutions of a system of linear equations as explained before. However, the aforementioned trend is different for the QSPR-LSSVM nonlinear model, which depends on the radial basis of the support vector machine method;¹⁶¹ 2. The random allocations of the data through subdata sets may result in different trends for representation/prediction of the hydrate dissociation

Table 2. Statistical Parameters of the QSPR-LSSVM Non-linear Model^a

statistical parameter	value
Training Set	
R^2	0.992
absolute average relative deviation ^b , %	3.4
standard deviation error	0.22
root mean square error	0.22
N^c	206
Validation Set	
R^2	0.993
absolute average relative deviation, %	6.8
standard deviation error	0.24
root mean square error	0.24
N	44
Test Set	
R^2	0.994
absolute average relative deviation, %	5.0
standard deviation error	0.21
root mean square error	0.21
N	44
Training + Validation + Test Set	
R^2	0.992
absolute average relative deviation, %	3.9
standard deviation error	0.08
root mean square error	0.22
N	294

^a R^2 = squared correlation coefficient. ^b %AARD = $(100/(N - n)) \sum_i^N (|Rep.(i)/Pred.(i) - Exp.(i)| / Exp.(i))$, where n is the number of the model parameters. ^c Number of experimental data.

conditions. Therefore, one datum may be used in training set in the first model while it may be applied in validation or test sets in the second one; 3. In this work, we are dealing with a parameter (hydrate dissociation pressure) that we are almost confident about its nonlinear relationship with the physical properties of the promoters such as critical temperature and critical pressure (the previously proposed nonlinear thermodynamic models for this purpose demonstrate this fact). Therefore, it may be concluded that a nonlinear relationship between the hydrate dissociation pressure and physicochemical characteristics (molecular descriptors) may lead to much better accuracy of the results especially for the hydrate dissociation pressures with more different behaviors as function of temperatures than the others; 4. Finally and perhaps the most importantly is the fact that in linear regression procedures, the accumulation of most of the points, used in regression, defines the general trend of the results obtained from the final relation between inputs and outputs of the calculation procedure. However, in algorithms such as LSSVM,¹⁶¹ accumulations of the data points are distributed in a continuous feasible region. Therefore, the trends of the results are not defined only by a single accumulation of the input data. As a result, the QSPR-LSSVM model may occasionally lead to very different hydrate dissociation values in comparison with the linear QSPR-GA-MLR model.

On the other hand, the deviations of the calculated/estimated hydrate dissociation pressures generally increase with increasing the temperature. Furthermore, we may not be able to define a

Table 3. Determined Hydrate Dissociation Conditions and Absolute Relative Deviations of the Obtained Results Using the Final Two Developed Models from Experimental Values^{129–145}

promoter	P^a /MPa	T^b /K	QSPR-GA-MLR linear model		QSPR-LSSVM nonlinear model	
			$P^{\text{Rep./Pred.}}$ /MPa	ARD % ^c	$P^{\text{Rep./Pred.}}$ /MPa	ARD %
2-methylbutane	2.654	275.2	2.49	6.2	2.678	0.9
	2.978	276.2	2.747	7.8	2.982	0.1
	3.64	277.8	3.262	10	3.560	2.2
	4.15	279	3.738	9.9	4.085	1.6
	2.241	274	2.229	0.5	2.359	5.3
	2.955	276.2	2.748	7.0	2.982	0.9
	3.501	277.4	3.114	11	3.403	2.8
2,2-dimethylpropane	0.4	276.6	0.801	100	0.732	83
	1.014	282.9	0.996	1.8	1.021	0.7
	1.593	286	1.166	27	1.935	21
	2.944	289.9	1.479	50	3.557	21
	4.861	292.8	2.133	56	4.859	0.0
2,2-dimethylbutane	1.598	276	1.615	1.1	1.605	0.4
	2.028	278	1.898	6.4	2.048	1.0
	2.391	279.2	2.105	12	2.385	0.3
	3.339	282.2	2.813	16	3.502	4.9
	5.22	285.4	4.086	22	5.198	0.4
	7.51	288.2	6.043	20	7.129	5.1
	1.415	275	1.498	5.9	1.432	1.2
	1.805	276.8	1.719	4.8	1.766	2.2
	2.601	279.9	2.243	14	2.609	0.3
	3.75	282.8	3.009	20	3.778	0.7
	0.332	244.8	0.354	6.6	0.351	5.7
	0.447	251.4	0.441	1.3	0.412	7.8
	0.626	258.8	0.595	5.0	0.664	6.1
	1.241	274	1.394	12	1.287	3.7
	0.509	254.4	0.494	2.9	0.516	1.4
	0.548	255.9	0.525	4.2	0.570	4.0
	0.597	257.85	0.57	4.5	0.636	6.5
	0.623	258.85	0.595	4.5	0.666	6.9
	0.678	260.85	0.653	3.7	0.717	5.8
	0.751	263.35	0.737	1.9	0.764	1.7
0.882	267.35	0.912	3.4	0.835	5.3	
0.966	269.65	1.046	8.3	0.916	5.2	
2,3-dimethylbutane	1.025	271.35	1.165	14	1.019	0.6
	1.095	272.85	1.284	17	1.152	5.2
	2.078	275.9	1.998	3.8	2.133	2.6
	2.482	277.4	2.289	7.8	2.497	0.6
	3.088	279.2	2.716	12	3.101	0.4
	3.795	280.8	3.237	15	3.826	0.8
	4.95	282.6	3.975	20	4.895	1.1
	8.19	286.4	6.885	16	8.161	0.4
2,2,3-trimethylbutane	1.475	275.6	1.605	8.8	1.618	9.7
	1.84	277.4	1.855	0.8	1.874	1.8
	2.247	279.5	2.231	0.7	2.248	0.0
	2.702	280.9	2.549	5.7	2.573	4.8
	5.94	288	6.185	4.1	6.185	4.1
	7.55	289.4	7.824	3.6	7.416	1.8
2,2-dimethylpentane	3.287	275.9	2.383	28	2.602	21
	3.819	277.4	2.763	28	3.297	14
	4.556	279.2	3.356	26	4.114	9.7

Table 3. Continued

promoter	P^a /MPa	T^b /K	QSPR-GA-MLR linear model		QSPR-LSSVM nonlinear model	
			$P^{\text{Rep./Pred.}}$ /MPa	ARD % ^c	$P^{\text{Rep./Pred.}}$ /MPa	ARD %
	5.14	280.31	3.825	26	4.611	10
	5.832	281.34	4.355	25	5.073	13
	6.195	282.2	4.916	21	5.468	12
	6.691	282.8	5.353	20	5.751	14
	3.79	286.6	eliminated		eliminated	
	5.7	288.2	eliminated		eliminated	
	7.15	290	eliminated		eliminated	
	1.734	274.8	2.18	26	2.092	21
	2.264	277	2.68	18	3.112	37
	3.009	279.2	3.385	12	4.114	37
	3.93	281.3	4.368	11	5.055	29
	3.62	280.6	3.995	10	4.740	31
	5.42	283.6	6.049	12	6.144	13
	7.28	286.4	9.926	36	7.752	6.5
methylcyclopentane	2.199	276.5	2.444	11	2.225	1.2
	2.578	277.8	2.779	7.8	2.646	2.6
	3.195	279.5	3.335	4.4	3.296	3.2
	3.812	280.8	3.884	1.9	3.895	2.2
	3.22	279.2	3.222	0.1	3.172	1.5
	3.94	281.3	4.136	5.0	4.153	5.4
	4.7	282.6	4.914	4.6	4.913	4.5
	6.14	284.8	6.86	12	6.531	6.4
	7.44	286	8.46	14	7.614	2.3
	8.69	287.2	10.715	23	8.842	1.7
	10.01	287.8	12.191	22	9.510	5.0
	2.635	278.2	2.897	9.9	2.788	5.8
	2.937	278.6	3.019	2.8	2.936	0.0
	2.965	279	3.155	6.4	3.091	4.2
	3.289	279.7	3.412	3.7	3.382	2.8
	3.737	280.35	3.678	1.6	3.676	1.6
	4.606	282.2	4.649	0.9	4.665	1.3
	4.999	283	5.198	4.0	5.174	3.5
	5.295	283.2	5.346	1.0	5.310	0.3
	6.653	285.2	7.336	10	6.876	3.4
	8.625	287	10.273	19	8.628	0.0
	1.75	274.28	2	14	1.619	7.5
	1.98	275.25	2.173	9.7	1.869	5.6
	2.22	276.2	2.374	6.9	2.136	3.8
	2.48	277.08	2.583	4.2	2.406	3.0
	2.77	277.99	2.83	2.2	2.712	2.1
	3.08	278.88	3.112	1.0	3.044	1.2
	3.47	279.78	3.441	0.8	3.417	1.5
	3.88	280.67	3.822	1.5	3.830	1.3
	4.29	281.48	4.229	1.4	4.251	0.9
	4.75	282.27	4.693	1.2	4.707	0.9
	5.25	283.06	5.239	0.2	5.214	0.7
	5.79	283.86	5.9	1.9	5.784	0.1
	6.44	284.66	6.691	3.9	6.414	0.4
	7.12	285.43	7.627	7.1	7.081	0.5
	7.92	286.21	8.79	11	7.818	1.3
	8.57	286.77	9.802	14	8.385	2.2
	9.34	287.4	11.171	20	9.061	3.0

Table 3. Continued

promoter	P^a /MPa	T^b /K	QSPR-GA-MLR linear model		QSPR-LSSVM nonlinear model	
			$P^{\text{Rep./Pred.}}$ /MPa	ARD % ^c	$P^{\text{Rep./Pred.}}$ /MPa	ARD %
methylcyclohexane	1.599	275.6	1.851	16	1.763	10
	2.137	277.6	2.198	2.9	2.197	2.8
	2.688	279.4	2.608	3.0	2.678	0.4
	3.357	281.2	3.149	6.2	3.289	2.0
	3	280.2	2.829	5.7	2.930	2.3
	3.2	280.6	2.95	7.8	3.067	4.2
	6	285.6	5.526	7.9	5.768	3.9
	10.2	289.6	11.306	11	9.889	3.0
	11.2	290.4	13.566	21	10.941	2.3
	3.99	282.6	3.701	7.2	3.895	2.4
	4.62	284.2	4.539	1.8	4.781	3.5
	6.47	286.45	6.303	2.6	6.478	0.1
	7.61	287.4	7.38	3.0	7.377	3.1
	8.82	289.2	10.406	18	9.389	6.5
	10.5	290.25	13.042	24	10.739	2.3
	2.041	277.1	2.1	2.9	2.080	1.9
	2.951	279.9	2.742	7.1	2.832	4.0
	3.937	282.2	3.528	10	3.708	5.8
	4.606	283.4	4.089	11	4.309	6.4
	7.391	287.1	7.01	5.2	7.081	4.2
	2.65	279.48	2.629	0.8	2.702	2.0
	2.93	280.49	2.919	0.4	3.029	3.4
	3.17	281.43	3.235	2.1	3.380	6.6
	3.87	282.42	3.623	6.4	3.809	1.6
	4.37	283.39	4.081	6.6	4.304	1.5
	4.81	284.44	4.689	2.5	4.936	2.6
	5.2	284.95	5.034	3.2	5.283	1.6
	5.5	285.44	5.401	1.8	5.644	2.6
	5.96	285.95	5.832	2.1	6.050	1.5
	6.34	286.49	6.348	0.1	6.514	2.7
	6.75	286.96	6.853	1.5	6.946	2.9
	7.34	287.46	7.461	1.6	7.437	1.3
	8.33	288.4	8.852	6.3	8.445	1.4
	9.13	288.97	9.908	8.5	9.110	0.2
	1.42	274.09	1.64	15	1.493	5.1
	1.54	274.78	1.73	12	1.611	4.6
	1.66	275.28	1.801	8.5	1.702	2.5
	1.75	275.79	1.876	7.2	1.801	2.9
	1.87	276.26	1.953	4.4	1.896	1.4
	1.99	276.79	2.044	2.7	2.010	1.0
2.11	277.26	2.131	1.0	2.116	0.3	
2.25	277.8	2.238	0.5	2.245	0.2	
2.39	278.3	2.344	1.9	2.372	0.8	
2.7	279.25	2.568	4.9	2.634	2.4	
3.05	280.26	2.847	6.7	2.950	3.3	
3.45	281.27	3.174	8.0	3.316	3.9	
3.9	282.28	3.563	8.6	3.744	4.0	
4.43	283.29	4.029	9.1	4.249	4.1	
5.03	284.3	4.601	8.5	4.845	3.7	
5.72	285.29	5.28	7.7	5.531	3.3	
6.5	286.28	6.133	5.6	6.329	2.6	
7.42	287.25	7.191	3.1	7.227	2.6	

Table 3. Continued

promoter	P^a /MPa	T^b /K	QSPR-GA-MLR linear model		QSPR-LSSVM nonlinear model	
			$P^{\text{Rep./Pred.}}$ /MPa	ARD % ^c	$P^{\text{Rep./Pred.}}$ /MPa	ARD %
	8.48	288.29	8.666	2.2	8.322	1.9
	0.519	251.5	0.48	7.5	0.525	1.2
	0.559	253.15	0.512	8.4	0.539	3.6
	0.619	255.7	0.57	7.9	0.634	2.4
	0.686	258.1	0.634	7.6	0.745	8.6
	0.774	261	0.729	5.8	0.832	7.5
	0.873	264	0.853	2.3	0.852	2.4
	0.984	267	1.012	2.8	0.872	11
	1.063	269.05	1.15	8.2	0.945	11
	1.145	271	1.309	14	1.091	4.7
	1.213	272.6	1.467	21	1.273	4.9
<i>cis</i> -1,2-dimethylcyclohexane	1.871	275.8	1.861	0.5	1.899	1.5
	2.237	277.4	2.136	4.5	2.308	3.2
	2.816	279.4	2.579	8.4	2.932	4.1
	3.433	281	3.049	11	3.553	3.5
	4	282	3.403	15	4.017	0.4
	5.29	284.4	4.601	13	5.449	3.0
	6.81	286.2	5.955	13	6.895	1.2
	7.63	287.4	7.257	4.9	8.064	5.7
	9.67	288.8	9.369	3.1	9.636	0.4
	11.32	290	12.065	6.6	11.151	1.5
	1.57	274.18	1.634	4.1	1.552	1.1
	1.67	274.65	1.695	1.5	1.646	1.4
	1.8	275.25	1.778	1.2	1.774	1.4
	2.03	276.22	1.926	5.1	2.000	1.5
	2.29	277.18	2.096	8.5	2.248	1.8
	2.57	278.14	2.283	11	2.523	1.8
	2.89	279.1	2.501	13	2.829	2.1
	3.28	280.1	2.765	16	3.188	2.8
	3.93	281.58	3.243	17	3.814	3.0
	4.71	283.04	3.849	18	4.576	2.8
	5.66	284.53	4.671	17	5.541	2.1
	6.83	285.99	5.765	16	6.708	1.8
	7.75	286.93	6.691	14	7.586	2.1
	8.89	287.96	7.993	10	8.666	2.5
2,3-dimethyl-1-butene	2.53	275.7	2.751	8.7	2.576	1.8
	3.275	277.8	3.438	5.0	3.217	1.8
	4.088	279.53	4.23	3.5	4.042	1.1
	4.805	280.78	4.996	4.0	4.839	0.7
3,3-dimethyl-1-butene	2.016	276.2	2.009	0.3	2.027	0.6
	2.423	277.6	2.273	6.2	2.359	2.6
	2.933	279.2	2.659	9.3	2.891	1.4
	3.871	281.42	3.357	13	3.909	1.0
3,3-dimethyl-1-butyne	2.851	275.8	2.725	4.4	2.852	0.0
	3.216	276.9	3.053	5.1	3.278	1.9
	3.878	278.4	3.641	6.1	3.935	1.5
	4.133	278.9	3.824	7.5	4.170	0.9
	4.567	279.6	4.162	8.9	4.510	1.2
cycloheptene	2.106	275.1	1.984	5.8	2.164	2.8
	2.671	277.7	2.524	5.5	2.629	1.6
	3.051	279.2	2.941	3.6	3.014	1.2
	3.809	281	3.597	5.6	3.655	4.0

Table 3. Continued

promoter	P^a /MPa	T^b /K	QSPR-GA-MLR linear model		QSPR-LSSVM nonlinear model	
			$P^{\text{Rep./Pred.}}$ /MPa	ARD % ^c	$P^{\text{Rep./Pred.}}$ /MPa	ARD %
<i>cis</i> -cyclooctene	2.082	276.9	2.683	29	1.999	4.0
	2.562	278.5	3.16	23	2.484	3.0
	3.009	280	3.766	25	3.073	2.1
	3.561	281.3	4.419	24	3.719	4.4
adamantane	1.779	275.1	1.738	2.3	1.598	10
	2.165	276.9	2.02	6.7	2.103	2.9
	2.51	278.4	2.315	7.8	2.544	1.4
	3.001	280.2	2.761	8.0	3.106	3.5
	1.79	275.2	1.752	2.1	1.625	9.2
	1.941	275.9	1.855	4.4	1.819	6.3
	2.3	277.6	2.149	6.6	2.307	0.3
	2.709	279.1	2.473	8.7	2.757	1.8
ethylcyclopentane	3.59	280.2	3.565	0.7	3.607	0.5
	4.02	281.2	4.024	0.1	4.044	0.6
	5.16	283.2	5.263	2.0	5.181	0.4
	6.39	284.8	6.722	5.2	6.404	0.2
	7.93	286.4	8.932	13	7.954	0.3
	9.13	287.4	10.921	20	9.099	0.3
1,1-dimethylcyclohexane	2	280.2	2.179	8.9	2.266	13
	2.34	281	2.346	0.3	2.471	5.6
	2.82	282.4	2.693	4.5	2.855	1.2
	3.34	283.6	3.057	8.5	3.235	3.1
	4.3	285.8	3.96	7.9	4.150	3.5
	5.51	287.8	5.196	5.7	5.347	3.0
	6.06	288.8	6.043	0.3	6.106	0.8
	7.53	290.6	8.22	9.2	7.760	3.1
	9.07	291.8	10.413	15	9.053	0.2
	10.13	292.6	12.416	23	9.985	1.4
	11.53	293.2	14.24	24	10.714	7.1
	1.07	274.67	1.398	31	0.848	21
	1.37	276.67	1.619	18	1.370	0.0
	1.76	278.65	1.9	8.0	1.877	6.6
	2.19	280.63	2.265	3.4	2.376	8.5
	2.9	282.61	2.751	5.1	2.918	0.6
3.74	284.57	3.412	8.8	3.597	3.8	
4.75	286.53	4.351	8.4	4.540	4.4	
6.08	288.51	5.773	5.0	5.874	3.4	
6.77	289.31	6.558	3.1	6.538	3.4	
<i>cis</i> -1,4-dimethylcyclohexane	1.62	274.13	1.856	15	1.602	1.1
	1.76	274.75	1.959	11	1.727	1.9
	1.88	275.3	2.053	9.2	1.849	1.6
	2.03	275.98	2.181	7.4	2.014	0.8
	2.24	276.79	2.348	4.8	2.233	0.3
	2.46	277.55	2.524	2.6	2.459	0.0
	2.79	278.57	2.795	0.2	2.797	0.3
	3.14	279.53	3.095	1.4	3.155	0.5
	3.53	280.5	3.451	2.2	3.561	0.9
	3.93	281.44	3.858	1.8	4.002	1.8
	4.22	281.97	4.121	2.3	4.275	1.3
	4.45	282.45	4.384	1.5	4.539	2.0
	5.01	283.43	5.009	0.0	5.130	2.4
	5.62	284.3	5.685	1.2	5.720	1.8

Table 3. Continued

promoter	P^a /MPa	T^b /K	QSPR-GA-MLR linear model		QSPR-LSSVM nonlinear model	
			$P^{\text{Rep./Pred.}}$ /MPa	ARD % ^c	$P^{\text{Rep./Pred.}}$ /MPa	ARD %
	6.32	285.3	6.649	5.2	6.482	2.6
	6.78	285.72	7.13	5.2	6.831	0.8
	7.16	286.15	7.673	7.2	7.206	0.6
	8.04	286.97	8.927	11	7.974	0.8
	8.53	287.49	9.889	16	8.497	0.4
	9.13	287.95	10.871	19	8.983	1.6
ethylcyclohexane	6.3	283.6	6.387	1.4	6.423	2.0
	8.9	286	9.784	9.9	8.659	2.7
cycloheptane	3.39	281.4	3.043	10	3.110	8.3
	4.62	284.1	4.187	9.4	4.490	2.8
	5.15	285	4.72	8.3	5.099	1.0
	6.54	286.8	6.148	6.0	6.598	0.9
	7.79	288.2	7.781	0.1	8.043	3.2
	9.15	289.2	9.381	2.5	9.227	0.8
	10.93	290.4	12.073	10	10.801	1.2
cyclooctane	4.21	282.4	4.156	1.3	4.225	0.4
	5.36	284.4	5.469	2.0	5.433	1.4
	6.29	285.8	6.803	8.2	6.507	3.4
	6.63	286.4	7.56	14	7.031	6.0
	7.55	287.4	eliminated		eliminated	
	9.65	289	9.089	5.8	7.994	17
	11.65	290.4	12.728	9.3	9.762	16
	1.6	274.08	1.8	13	1.665	4.1
	1.84	275.16	1.962	6.6	1.858	1.0
	2.03	276.17	2.147	5.8	2.069	1.9
	2.29	277.15	2.346	2.4	2.302	0.5
	2.53	278	2.545	0.6	2.529	0.0
	2.79	278.83	2.765	0.9	2.776	0.5
	3.14	279.78	3.054	2.7	3.094	1.5
	3.57	280.96	3.487	2.3	3.551	0.5
	4.13	282.13	4.016	2.8	4.088	1.0
	4.64	283.07	4.539	2.2	4.591	1.1
	5.28	284.11	5.241	0.7	5.235	0.9
	5.83	284.9	5.897	1.1	5.793	0.6
	6.59	285.9	6.914	4.9	6.592	0.0
	7.5	286.91	8.272	10	7.508	0.1
	8.53	287.87	9.908	16	8.485	0.5
	8.84	288.13	10.5	19	8.767	0.8
	9.33	288.57	11.538	24	9.260	0.8
overall				9.0		3.9

^a P = pressure. ^b T = temperature. ^c %ARD = $100 \sum_i^N (|(\text{Rep.}(i))/(\text{Pred.}(i) - \text{Exp.}(i))|)/(\text{Exp.}(i))$.

branch of hydrate promoters, for which the developed models lead to obtaining poorer or better results in comparison with other groups of the investigated heavy hydrocarbon promoters. However, consistent experimental clathrate hydrate dissociation data generally shows a straight line behavior in semilogarithmic pressure–temperature diagram. Consequently, we may doubt some of the experimental data regarding 2,2-dimethylpentane hydrate former based on this phenomenon. These plots are reported in Supporting Information excel file. Our developed models also show high deviations for the corresponding hydrate dissociation data.

Another element to consider is that we have tried to use almost all of available corresponding experimental data^{129–145} in open literature. However, several error sources in experimental measurements including calibration of pressure transducers, temperature probes, and possible errors during the measurements of phase equilibria such as improper design of the equipment, insufficient experimental time to pass the metastable region, etc.^{175–177} may lead to generate unreliable experimental data and consequently contribute to decrease the accuracy and prediction capability of the developed models.

4. CONCLUSION

Two novel molecular models have been presented for determination of hydrate phase equilibria of the systems containing water “insoluble” hydrocarbon promoter + methane + water. Twenty-one promoters were examined for this purpose. The experimental data^{129–145} reported in open literature were applied for developing and testing the models. The genetic-algorithm-based multivariate linear regression^{150,151} (GA-MLR) was used to select the most appropriate model parameters (molecular descriptors) from a domain of descriptors. The required parameters of the linear model are the numbers of 5 molecular descriptors in each investigated molecule (promoter). The least-squares support vector machines¹⁶¹ (LSSVM) mathematical tool was applied to present a more accurate nonlinear model. Furthermore, the pattern search hybrid genetic algorithm (H-GA)^{167,168} optimization method was implemented to optimize the LSSVM¹⁶¹ model performance. The statistical parameters of the obtained models show that they are reliable, comprehensive, and predictive tools in order to represent/predict the sH hydrate dissociation conditions for the methane + water “insoluble” hydrocarbon promoter + water system, which are especially applicable in gas storage processes. Another issue to point out is the effect of uncertainties of the experimental data, applied for developing the model, on the obtained predicted results that cannot be ignored. It is undoubtedly possible to develop more accurate and predictive methods in the case of availability of more reliable phase equilibrium data.

■ APPENDIX A. INSTRUCTION FOR RUNNING THE PROGRAM

To run the program, developed based on the QSPR-LSSVM model, the LSSVM toolbox developed for MATLAB is required.¹⁶² First, one should insert the directory of the toolbox as the main directory in MATLAB. Later, it is required to drag and drop the model .mat file into the MATLAB workspace.

Example:

Calculation of the clathrate hydrate dissociation pressure of 2-methylbutane at 275.2 K

First, calculate and enter the molecular descriptors for 2-methylbutane at 275.2 (see the Supporting Information XLS file). The set of molecular descriptors are as follows:

```
EEig07d ([E]ij)  Mor12v  E1u  T^2  HATS4u^2
0                -0.49  0.514  75735.04  1.990921
```

The hydrate dissociation pressure is then calculated simply using the below command line:

```
P_calc=simlssvm({trainV.P',trainV.T',type,gam,sig2,'RBF_kernel',
'preprocess'},{alpha,b},[0 -0.49 0.514 75735.04 1.990921])
```

The output result of the model will be 2.61 MPa. The corresponding experimental value is 2.65 MPa.

■ ASSOCIATED CONTENT

● **Supporting Information.** Detailed results of the two final developed models accompanied with the molecular descriptors present in each organic promoter in XLS format, the detailed equations of the applied mathematical algorithms in DOC format, and the developed computer program in MAT format. This material is available free of charge via the Internet at <http://pubs.acs.org>.

■ AUTHOR INFORMATION

Corresponding Author

*E-mail: amir-hossein.mohammadi@mines-paristech.fr. Tel.: + (33) 1 64 69 49 70. Fax: + (33) 1 64 69 49 68.

■ ACKNOWLEDGMENT

The financial supports of the ANR (Agence Nationale de la Recherche) and OSEM (Orientation Stratégique des Ecoles des Mines) are gratefully acknowledged. A.E. thanks MINES ParisTech for providing a Ph.D. scholarship.

■ REFERENCES

- (1) Sloan, E. D.; Koh, C. A. *Clathrate Hydrates of Natural Gases*, 3rd ed.; CRC Press, Taylor & Francis Group: Boca Raton, FL, 2008.
- (2) Belandria, V.; Eslamimanesh, A.; Mohammadi, A. H.; Théveneau, P.; Legendre, H.; Richon, D. Compositional analysis and hydrate dissociation conditions measurements for carbon dioxide + methane + water system. *Ind. Eng. Chem. Res.* **2011**, *50*, 5783–5794.
- (3) Eslamimanesh, A.; Mohammadi, A. H.; Richon, D. An improved Clapeyron model for predicting liquid water-hydrate-liquid hydrate former phase equilibria. *Chem. Eng. Sci.* **2011**, *66*, 1759–1764.
- (4) Belandria, V.; Eslamimanesh, A.; Mohammadi, A. H.; Richon, D. Gas hydrate formation in carbon dioxide + nitrogen + water system: Compositional analysis of equilibrium phases. *Ind. Eng. Chem. Res.* **2011**, *50*, 4722–4730.
- (5) Mohammadi, A. H.; Richon, D. Gas hydrate phase equilibrium in the presence of ethylene glycol or methanol aqueous solution. *Ind. Eng. Chem. Res.* **2010**, *49*, 8865–8869.
- (6) Mohammadi, A. H.; Richon, D. Methane hydrate phase equilibrium in the presence of salt (NaCl, KCl, or CaCl₂) + ethylene glycol or salt (NaCl, KCl, or CaCl₂) + methanol aqueous solution: Experimental determination of dissociation condition. *J. Chem. Thermodyn.* **2009**, *41*, 1374–1377.
- (7) Carroll, J. *Natural Gas Hydrates, A Guide for Engineers*, 2nd ed.; Gulf Professional Publishing: Burlington, MA, 2009.
- (8) Hammerschmidt, E. G. Formation of gas hydrates in natural gas transmission lines. *Ind. Eng. Chem.* **1934**, *26*, 851–5.
- (9) Belandria, V.; Eslamimanesh, A.; Mohammadi, A. H.; Richon, D. Study of gas hydrate formation in carbon dioxide + hydrogen + water system: Compositional analysis of gas phase. *Ind. Eng. Chem. Res.* **2011**, *50*, 6455–6459.
- (10) Sun, C.; Li, W.; Yang, X.; Li, F.; Yuan, Q.; Mu, L.; Chen, J.; Liu, B.; Chen, G. Progress in Research of Gas Hydrate. *Chin. J. Chem. Eng.* **2011**, *19*, 151–162.
- (11) Lang, X.; Fan, S.; Wang, Y. Intensification of methane and hydrogen storage in clathrate hydrate and future prospect. *J. Nat. Gas Chem.* **2011**, *19*, 203–209.
- (12) Celzard, A.; Fierro, V. Preparing a suitable material designed for methane storage: A comprehensive report. *Energy Fuels* **2005**, *19*, 573–583.
- (13) Di Profio, P.; Arca, S.; Germani, R.; Savelli, G. Novel nanostructured media for gas storage and transport: Clathrate hydrates of methane and hydrogen. *Fuel Sci. Technol. Int.* **2007**, *4*, 49–55.
- (14) Guo, Y. K.; Fan, S. S.; Guo, K. H.; Chen, Y. Methane storage in hydrate form using calcium hypochlorite as additive. *Proceedings of the Fourth International Conference on Natural Gas Hydrates*; Yokohama, Japan, 1040–1043, 2002.
- (15) Ganji, H.; Manteghian, M.; Rahimi Mofrad, H. Effect of mixed compounds on methane hydrate formation and dissociation rates and storage capacity. *Fuel Process. Technol.* **2007**, *88*, 891–895.
- (16) Ganji, H.; Manteghian, M.; Sadaghiani Zadeh, K.; Omidkhah, M. R.; Rahimi Mofrad, H. Effect of different surfactants on methane hydrate formation rate, stability and storage capacity. *Fuel* **2007**, *86*, 434–441.

- (17) Hao, W.; Wang, J.; Fan, S. Evaluation and analysis method for natural gas hydrate storage and transportation processes. *Energy Conversion Management* **2008**, *49*, 2546–2553.
- (18) Khokhar, A. A.; Gudmundsson, J. S.; Sloan, E. D. Gas storage in structure H hydrates. *Fluid Phase Equilib.* **1998**, *150*, 383–392.
- (19) Khokhar, A. A.; Sloan, E. D.; Gudmundsson, J. S., Natural gas storage properties of structure H hydrate. In *Gas Hydrates: Challenges For The Future*, **2000**.
- (20) Kroon, M. C.; Docherty, H.; Cummings, P. T.; Peters, C. J.; Mao, W. L. Discovery of a new mixed methane-hydrogen hydrate phase with very high hydrogen storage capacity, 2010 AIChE Annual Meeting, Conference Proceedings, 2010.
- (21) Kumar, R.; Linga, P.; Moudrakovski, I.; Ripmeester, J. A.; Englezos, P. Structure and kinetics of gas hydrates from methane/ethane/propane mixtures relevant to the design of natural gas hydrate storage and transport facilities. *AIChE J.* **2008**, *54*, 2132–2144.
- (22) Lang, X.; Fan, S.; Wang, Y. Intensification of methane and hydrogen storage in clathrate hydrate and future prospect. *J. Nat. Gas Chem.* **2010**, *19*, 203–209.
- (23) Masoudi, R.; Tohidi, B. In Gas hydrate production technology for natural gas storage and transportation and CO₂ sequestration. SPE 93492, the 14th Middle East Oil & Gas Show and Conference, Kingdom of Bahrain, 12–15 March, 2005.
- (24) Pang, W. X.; Chen, G. J.; Dandekar, A.; Sun, C. Y.; Zhang, C. L. Experimental study on the scale-up effect of gas storage in the form of hydrate in a quiescent reactor. *Chem. Eng. Sci.* **2007**, *62*, 2198–2208.
- (25) Peng, X.; Zhou, J.; Wang, W.; Cao, D. Computer simulation for storage of methane and capture of carbon dioxide in carbon nanoscrolls by expansion of interlayer spacing. *Carbon* **2010**, *48*, 3760–3768.
- (26) Perrin, A.; Celzard, A.; Mardché, J. F.; Furdin, G. Methane storage within dry and wet active carbons: A comparative study. *Energy Fuels* **2003**, *17*, 1283–1291.
- (27) Savelli, G.; Di Profio, P.; Arca, S.; Germani, R. In Novel nanostructured media for gas storage and transport: Clathrate hydrates of methane and hydrogen. Proceedings of the 1st European Fuel Cell Technology and Applications Conference 2005 - Book of Abstracts 2005, 240.
- (28) Seo, Y.; Lee, J. W.; Kumar, R.; Moudrakovski, I. L.; Lee, H.; Ripmeester, J. A. Tuning the composition of guest molecules in clathrate hydrates: NMR identification and its significance to gas storage. *Chem. –Asian J.* **2009**, *4*, 1266–1274.
- (29) Seo, Y. T.; Lee, H. ¹³C NMR Analysis and gas uptake measurements of pure and mixed gas hydrates: Development of natural gas transport and storage method using gas hydrate. *Korean J. Chem. Eng.* **2003**, *20*, 1085–1091.
- (30) Sun, Z.; Ma, R.; Fan, S.; Guo, K.; Wang, R. Investigation on gas storage in methane hydrate. *J. Nat. Gas Chem.* **2004**, *13*, 107–112.
- (31) Sun, Z. G.; Ma, R. S.; Wang, R. Z.; Guo, K. H.; Fa, S. S. Experimental studying of additives effects on gas storage in hydrates. *Energy Fuels* **2003**, *17*, 1180–1185.
- (32) Sun, Z. G.; Wang, R.; Ma, R.; Guo, K.; Fan, S. Natural gas storage in hydrates with the presence of promoters. *Energ. Convers. Manage.* **2003**, *44*, 2733–2742.
- (33) Tulk, C. A.; Wright, J. F.; Ratcliffe, C. I.; Ripmeester, J. A. Storage and handling of natural gas hydrate. *Bull. Geo. Survey Canada* **2003**, *544*, 263–267.
- (34) Uchida, T.; Ikeda, I. Y.; Takeya, S.; Kamata, Y.; Ohmura, R.; Nagao, J.; Zatssepina, O. Y.; Buffett, B. A. Kinetics and stability of CH₄-CO₂ mixed gas hydrates during formation and long-term storage. *ChemPhysChem* **2005**, *6*, 646–654.
- (35) Wang, W.; Bray, C. L.; Adams, D. J.; Cooper, A. I. Methane storage in dry water gas hydrates. *J. Am. Chem. Soc.* **2008**, *130*, 11608–11609.
- (36) Yevi, G. Y.; Rogers, R. E. Storage of fuel in hydrates for Natural Gas Vehicles (NGVs). *J. Energy Resources Technol., Trans. ASME* **1996**, *118*, 209–213.
- (37) Zheng, X.; Sun, Z.; Fan, S.; Zhang, C.; Guo, Y.; Guo, K. Experimental investigation of storage capacity of natural gas hydrate. *Tianranqi Gongye/Natural Gas Industry* **2003**, *23*, 95–97.
- (38) Kim, N. J.; Hwan Lee, J.; Cho, Y. S.; Chun, W. Formation enhancement of methane hydrate for natural gas transport and storage. *Energy* **2010**, *35*, 2717–2722.
- (39) Xie, Y.; Li, G.; Liu, D.; Liu, N.; Qi, Y.; Liang, D.; Guo, K.; Fan, S. Experimental study on a small scale of gas hydrate cold storage apparatus. *Appl. Energy* **2010**, *87*, 3340–3346.
- (40) Yang, L.; Fan, S. S.; Lang, X. M. Application prospects of gas hydrate as cool storage media in air-conditioning. *Xiandai Huagong/Modern Chemical Industry* **2008**, *28*, 33–37.
- (41) Bi, Y.; Guo, T.; Zhu, T.; Zhang, L.; Chen, L. Influences of additives on the gas hydrate cool storage process in a new gas hydrate cool storage system. *Energ. Convers. Manage.* **2006**, *47*, 2974–2982.
- (42) Papadimitriou, N. I.; Tsimpanogiannis, I. N.; Stubos, A. K.; Martín, A.; Rovetto, L. J.; Florusse, L. J.; Peters, C. J. Experimental and computational investigation of the sII Binary He-THF hydrate. *J. Phys. Chem. B* **2011**, *115*, 1411–1415.
- (43) Sabil, K. M.; Duarte, A. R. C.; Zevenbergen, J.; Ahmad, M. M.; Yusup, S.; Omar, A. A.; Peters, C. J. Kinetic of formation for single carbon dioxide and mixed carbon dioxide and tetrahydrofuran hydrates in water and sodium chloride aqueous solution. *Int. J. Greenh. Gas. Con.* **2010**, *4*, 798–805.
- (44) Sabil, K. M.; Witkamp, G. J.; Peters, C. J. Phase equilibria in ternary (carbon dioxide + tetrahydrofuran + water) system in hydrate-forming region: Effects of carbon dioxide concentration and the occurrence of pseudo-retrograde hydrate phenomenon. *J. Chem. Thermodyn.* **2010**, *42*, 8–16.
- (45) Mooijer-van den Heuvel, M. M.; Witterman, R.; Peters, C. J. Phase behaviour of gas hydrates of carbon dioxide in the presence of tetrahydropyran, cyclobutanone, cyclohexane and methylcyclohexane. *Fluid Phase Equilib.* **2001**, *182*, 97–110.
- (46) Strobel, T. A.; Hester, K. C.; Koh, C. A.; Sum, A. K.; Sloan, E. D., Jr. Properties of the clathrates of hydrogen and developments in their applicability for hydrogen storage. *Chem. Phys. Lett.* **2009**, *478*, 97–109.
- (47) Strobel, T. A.; Koh, C. A.; Sloan, E. D. Thermodynamic predictions of various tetrahydrofuran and hydrogen clathrate hydrates. *Fluid Phase Equilib.* **2009**, *280*, 61–67.
- (48) Shin, K.; Kim, Y.; Strobel, T. A.; Prasad, S. R.; Sugahara, T.; Lee, H.; Sloan, E. D.; Sum, A. K.; Koh, C. A. Tetra-n-butylammonium borohydride semiclathrate: A hybrid material for hydrogen storage. *J. Phys. Chem. A* **2009**, *113*, 6415–6418.
- (49) Eslamimanesh, A.; Mohammadi, A. H.; Blandria, V.; Richon, D. ANR SECOHYA project internal progress report, July 2010.
- (50) Acosta, H. Y.; Bishnoi, P. R.; Clarke, M. A. Experimental measurements of the thermodynamic equilibrium conditions of tetra-n-butylammonium bromide semiclathrates formed from synthetic landfill gases. *J. Chem. Eng. Data* **2011**, *56*, 69–73.
- (51) Lee, S.; Lee, Y.; Park, S.; Seo, Y. Phase equilibria of semiclathrate hydrate for nitrogen in the presence of tetra-n-butylammonium bromide and fluoride. *J. Chem. Eng. Data* **2010**, *55*, 5883–5886.
- (52) Uchida, T.; Shiga, T.; Nagayama, M.; Gohara, K. Observation of sintering of clathrate hydrates. *Energies* **2010**, *3*, 1960–1971.
- (53) Chapoy, A.; Gholinezhad, J.; Tohidi, B. Experimental clathrate dissociations for the hydrogen + water and hydrogen + tetrabutylammonium bromide + water systems. *J. Chem. Eng. Data* **2010**, *55*, 5323–5327.
- (54) Li, G.; Liu, D.; Xie, Y. Study on thermal properties of TBAB-THF hydrate mixture for cold storage by DSC. *J. Therm. Anal. Calorim.* **2010**, *102*, 819–826.
- (55) Oshima, M.; Shimada, W.; Hashimoto, S.; Tani, A.; Ohgaki, K. Memory effect on semi-clathrate hydrate formation: A case study of tetragonal tetra-n-butyl ammonium bromide hydrate. *Chem. Eng. Sci.* **2010**, *65*, 5442–5446.
- (56) Rodionova, T.; Komarov, V.; Villevald, G.; Aladko, L.; Karpova, T.; Manakov, A. Calorimetric and structural studies of tetrabutylammonium chloride ionic clathrate hydrates. *J. Phys. Chem. B* **2010**, *114*, 11838–11846.
- (57) Deschamps, J.; Dalmazzone, D. Hydrogen storage in semi-clathrate hydrates of tetrabutyl ammonium chloride and tetrabutyl phosphonium bromide. *J. Chem. Eng. Data* **2010**, *55*, 3395–3399.

- (58) Li, S.; Fan, S.; Wang, J.; Lang, X.; Wang, Y. Semiclathrate hydrate phase equilibria for CO₂ in the presence of tetra-n-butyl ammonium halide (bromide, chloride, or fluoride). *J. Chem. Eng. Data* **2010**, *55*, 3212–3215.
- (59) Sun, Z. G.; Sun, L. Equilibrium conditions of semi-clathrate hydrate dissociation for methane + tetra-n-butyl ammonium bromide. *J. Chem. Eng. Data* **2010**, *55*, 3538–3541.
- (60) Sugahara, T.; Haag, J. C.; Warntjes, A. A.; Prasad, P. S. R.; Sloan, E. D.; Koh, C. A.; Sum, A. K. Large-cage occupancies of hydrogen in binary clathrate hydrates dependent on pressures and guest concentrations. *J. Phys. Chem. C* **2010**, *114*, 15218–15222.
- (61) Li, X. S.; Xu, C. G.; Chen, Z. Y.; Wu, H. J. Tetra-n-butyl ammonium bromide semi-clathrate hydrate process for post-combustion capture of carbon dioxide in the presence of dodecyl trimethyl ammonium chloride. *Energy* **2010**, *35*, 3902–3908.
- (62) Li, X. S.; Xia, Z. M.; Chen, Z. Y.; Yan, K. F.; Li, G.; Wu, H. J. Equilibrium hydrate formation conditions for the mixtures of CO₂ + H₂ + tetrabutyl ammonium bromide. *J. Chem. Eng. Data* **2010**, *55*, 2180–2184.
- (63) Mayoufi, N.; Dalmazzone, D.; Fürst, W.; Delahaye, A.; Fournaison, L. CO₂ enclathration in hydrates of peralkyl-(Ammonium/Phosphonium) salts: Stability conditions and dissociation enthalpies. *J. Chem. Eng. Data* **2010**, *55*, 1271–1275.
- (64) Makino, T.; Yamamoto, T.; Nagata, K.; Sakamoto, H.; Hashimoto, S.; Sugahara, T.; Ohgaki, K. Thermodynamic stabilities of tetra-n-butyl ammonium chloride + H₂, N₂, CH₄, CO₂, or C₂H₆ semiclathrate hydrate systems. *J. Chem. Eng. Data* **2010**, *55*, 839–841.
- (65) Wenji, S.; Rui, X.; Chong, H.; Shihui, H.; Kaijun, D.; Ziping, F. Experimental investigation on TBAB clathrate hydrate slurry flows in a horizontal tube: Forced convective heat transfer behaviors. *Int. J. Refrig.* **2009**, *32*, 1801–1807.
- (66) Deschamps, J.; Dalmazzone, D. Dissociation enthalpies and phase equilibrium for TBAB semi-clathrate hydrates of N₂, CO₂, N₂ + CO₂ and CH₄ + CO₂. *J. Therm. Anal. Calorim.* **2009**, *98*, 113–118.
- (67) Fan, S.; Li, S.; Wang, J.; Lang, X.; Wang, Y. Efficient capture of CO₂ from simulated flue gas by formation of TBAB or TBAF semi-clathrate hydrates. *Energy Fuels* **2009**, *23*, 4202–4208.
- (68) Xiao, R.; Song, W.-J.; Huang, C.; He, S.-H.; Dong, K.-J.; Feng, Z.-P. Re-laminarization of TBAB hydrate slurry flow in tube. *Kung Cheng Je Wu Li Hsueh Pao/Journal of Engineering Thermophysics* **2009**, *30*, 971–973.
- (69) Schildmann, S.; Nowaczyk, A.; Geil, B.; Gainaru, C.; Böhmer, R. Water dynamics on the hydrate lattice of a tetrabutyl ammonium bromide semiclathrate. *J. Chem. Phys.* **2009**, *130*, 104505.
- (70) Li, S.; Fan, S.; Wang, J.; Lang, X.; Liang, D. CO₂ capture from binary mixture via forming hydrate with the help of tetra-n-butyl ammonium bromide. *J. Nat. Gas Chem.* **2009**, *18*, 15–20.
- (71) Ma, Q. L.; Chen, G. J.; Ma, C. F.; Zhang, L. W. Study of vapor-hydrate two-phase equilibria. *Fluid Phase Equilib.* **2008**, *265*, 84–93.
- (72) Kim, S. M.; Lee, J. D.; Lee, H. J.; Lee, E. K.; Kim, Y. Gas hydrate formation method to capture the carbon dioxide for pre-combustion process in IGCC plant. *Int. J. Hydrogen Energy* **2011**, *36*, 1115–1121.
- (73) Li, X. S.; Xu, C. G.; Chen, Z. Y.; Wu, H. J. Hydrate-based pre-combustion carbon dioxide capture process in the system with tetra-n-butyl ammonium bromide solution in the presence of cyclopentane. *Energy* **2011**, *36*, 1394–1403.
- (74) Kamata, Y.; Oyama, H.; Shimada, W.; Ebinuma, T.; Takeya, S.; Uchida, T.; Nagao, J.; Narita, H. Gas separation method using tetra-n-butyl ammonium bromide semi-clathrate hydrate. *Jpn. J. Appl. Phys., Part 1* **2004**, *43*, 362–365.
- (75) De Deugd, R. M.; Jager, M. D.; de Swaan Arons, J. Mixed hydrates of methane and water-soluble hydrocarbons modeling of empirical results. *AIChE J.* **2001**, *47*, 693–704.
- (76) Lee, S.; Yedlapalli, P.; Lee, J. W. Excess Gibbs potential model for multicomponent hydrogen clathrates. *J. Phys. Chem. B* **2006**, *110*, 26122–26128.
- (77) Seo, Y.-T.; Kang, S. P.; Lee, H. Experimental determination and thermodynamic modeling of methane and nitrogen hydrates in the presence of THF, propylene oxide, 1,4-dioxane and acetone. *Fluid Phase Equilib.* **2011**, *189*, 99–110.
- (78) Mainusch, S.; Peters, C. J.; de Swaan Arons, J.; Javanmardi, J.; Moshfeghian, M. Experimental determination and modeling of methane hydrates in mixtures of acetone and water. *J. Chem. Eng. Data* **1997**, *42*, 948–950.
- (79) Jager, M. D.; de Deugd, R. M.; Peters, C. J.; de Swaan Arons, J.; Sloan, E. D. Experimental determination and modeling of structure II hydrates in mixtures of methane + water +1,4-dioxane. *Fluid Phase Equilib.* **1999**, *165*, 209–223.
- (80) van der Waals, J. H.; Platteeuw, J. C. Clathrate solutions. *Adv. Chem. Phys.* **1959**, *2*, 1–57.
- (81) Kamran-Pirzaman, A.; Pahlavanzadeh, H.; Mohammadi, A. H. Thermodynamic model for prediction of pressure – temperature phase diagrams of clathrate hydrates of methane, carbon dioxide or nitrogen + tetrahydrofuran. Proceeding of the first National Iranian Conference on Gas Hydrate, Sharif University of Technology, Tehran, Iran, May 18-19, 2011.
- (82) Illbeigi, M.; Fazlali, A.; Mohammadi, A. H. Thermodynamic model for prediction of equilibrium conditions of clathrate hydrates of methane + water-soluble or -insoluble hydrate former. *Ind. Eng. Chem. Res.* **2011**, *50*, 9437–9450.
- (83) Mohammadi, A. H.; Richon, D. Hydrate phase equilibria for hydrogen + water and hydrogen + tetrahydrofuran + water systems: Predictions of dissociation conditions using an artificial neural network algorithm. *Chem. Eng. Sci.* **2010**, *65*, 3352–3355.
- (84) Mohammadi, A. H.; Martínez-López, J. F.; Richon, D. Determining phase diagrams of tetrahydrofuran+methane, carbon dioxide or nitrogen clathrate hydrates using an artificial neural network algorithm. *Chem. Eng. Sci.* **2010**, *65*, 6059–6063.
- (85) Mohammadi, A. H.; Beldandria, V.; Richon, D. Use of an artificial neural network algorithm to predict hydrate dissociation conditions for hydrogen + water and hydrogen + tetra-n-butyl ammonium bromide + water systems. *Chem. Eng. Sci.* **2010**, *65*, 4302–4305.
- (86) Paricaud, P. Modeling the dissociation conditions of salt hydrates and gas semiclathrate hydrates: application to lithium bromide, hydrogen iodide, and tetra-n-butylammonium bromide + carbon dioxide systems. *J. Phys. Chem. B* **2011**, *115*, 288–299.
- (87) Galindo, A.; Gil-Villegas, A.; Jackson, G.; Burgess, A. N. J. SAFT-VRE: Phase behavior of electrolyte solutions with the statistical associating fluid theory for potentials of variable range. *J. Phys. Chem. B* **1999**, *103*, 10272–10281.
- (88) Eslamimanesh, A.; Mohammadi, A. H.; Beldandria, V.; Richon, D. ANR SECOHYA project internal progress report, January 2011.
- (89) Mohammadi, A. H.; Richon, D. Equilibrium data of methyl cyclohexane + hydrogen sulfide and methyl cyclohexane + methane clathrate hydrates. *J. Chem. Eng. Data* **2010**, *55*, 566–569.
- (90) Mohammadi, A. H.; Richon, D. Phase equilibria of clathrate hydrates of cyclopentane + hydrogen sulfide and cyclopentane + methane. *Ind. Eng. Chem. Res.* **2009**, *48*, 9045–9048.
- (91) Mohammadi, A. H.; Richon, D. Clathrate hydrates of cyclohexane + hydrogen sulfide and cyclohexane + methane: Experimental measurements of dissociation conditions. *J. Chem. Eng. Data* **2010**, *55*, 1053–1055.
- (92) Mohammadi, A. H.; Richon, D. Clathrate hydrate dissociation conditions for the methane + cycloheptane/cyclooctane + water and carbon dioxide + cycloheptane/cyclooctane + water systems. *Chem. Eng. Sci.* **2010**, *65*, 3356–3361.
- (93) Mohammadi, A. H.; Richon, D. Phase equilibria of binary clathrate hydrates of nitrogen+cyclopentane/cyclohexane/methyl cyclohexane and ethane+cyclopentane/cyclohexane/methyl cyclohexane. *Chem. Eng. Sci.* doi:10.1016/j.ces.2011.06.014, **2011**.
- (94) Mooijer-van den Heuvel, M. M.; Peters, C. J. de Swaan Arons, J. Influence of water-insoluble organic components on the gas hydrate equilibrium conditions of methane. *Fluid Phase Equilib.* **2000**, *172*, 73–91.
- (95) Mooijer-van den Heuvel, M. M.; Witteman, R.; Peters, C. J. Phase behaviour of gas hydrates of carbon dioxide in the presence of tetrahydropyran, cyclobutanone, cyclohexane and methylcyclohexane. *Fluid Phase Equilib.* **2001**, *182*, 97–110.
- (96) Mohammadi, A. H.; Beldandria, V.; Richon, D. Can toluene or xylene form clathrate hydrates? *Ind. Eng. Chem. Res.* **2009**, *48*, 5916–5918.

- (97) Gharagheizi, F.; Eslamimanesh, A.; Mohammadi, A. H.; Richon, D. Use of artificial neural network-group contribution method to determine surface tension of pure compounds. *J. Chem. Eng. Data* **2011**, *56*, 2587–2601.
- (98) Gharagheizi, F.; Sattari, M. Prediction of triple-point temperature of pure components using their chemical structures. *Ind. Eng. Chem. Res.* **2010**, *49*, 929–932.
- (99) Gharagheizi, F.; Abbasi, R.; Tirandazi, B. Prediction of Henry's law constant of organic compounds in water from a new group-contribution-based model. *Ind. Eng. Chem. Res.* **2010**, *49*, 10149–10152.
- (100) Eslamimanesh, A.; Gharagheizi, F.; Mohammadi, A. H.; Richon, D. Artificial neural network modeling of solubility of supercritical carbon dioxide in 24 commonly used ionic liquids. *Chem. Eng. Sci.* **2011**, *66*, 3039–3044.
- (101) Gharagheizi, F.; Eslamimanesh, A.; Mohammadi, A. H.; Richon, D. Artificial neural network modeling of solubilities of 21 mostly-used industrial solid compounds in supercritical carbon dioxide. *Ind. Eng. Chem. Res.* **2011**, *50*, 221–226.
- (102) Gharagheizi, F.; Eslamimanesh, A.; Mohammadi, A. H.; Richon, D. Representation/prediction of solubilities of pure compounds in water using artificial neural network-group contribution method. *J. Chem. Eng. Data* **2011**, *56*, 720–726.
- (103) Gharagheizi, F.; Eslamimanesh, A.; Mohammadi, A. H.; Richon, D. QSPR approach for determination of parachor of non-electrolyte organic compounds. *Chem. Eng. Sci.* **2011**, *66*, 2959–2967.
- (104) Gharagheizi, F.; Eslamimanesh, A.; Mohammadi, A. H.; Richon, D. Determination of parachor of various compounds using an artificial neural network - group contribution method. *Ind. Eng. Chem. Res.* **2011**, *50*, 5815–5823.
- (105) Chouai, A.; Laugier, S.; Richon, D. Modeling of thermodynamic properties using neural networks: Application to refrigerants. *Fluid Phase Equilib.* **2002**, *199*, 53–62.
- (106) Piazza, L.; Scalabrin, G.; Marchi, P.; Richon, D. Enhancement of the extended corresponding states techniques for thermodynamic modelling. I. Pure fluids. *Int. J. Refrig.* **2006**, *29*, 1182–1194.
- (107) Scalabrin, G.; Marchi, P.; Bettio, L.; Richon, D. Enhancement of the extended corresponding states techniques for thermodynamic modelling. II. Mixtures. *Int. J. Refrig.* **2006**, *29*, 1195–1207.
- (108) Chapoy, A.; Mohammadi, A. H.; Richon, D. Predicting the hydrate stability zones of natural gases using Artificial Neural Networks. *Oil Gas Sci. Technol. – Rev. IFP* **2007**, *62*, 701–706.
- (109) Mohammadi, A. H.; Richon, D. Estimating sulfur content of hydrogen sulfide at elevated temperatures and pressures using an artificial neural network algorithm. *Ind. Eng. Chem. Res.* **2008**, *47*, 8499–8504.
- (110) Mohammadi, A. H.; Richon, D. A Mathematical model based on artificial neural network technique for estimating liquid water – hydrate equilibrium of water – hydrocarbon System. *Ind. Eng. Chem. Res.* **2008**, *47*, 4966–4970.
- (111) Mohammadi, A. H.; Afzal, W.; Richon, D. Determination of critical properties and acentric factors of petroleum fractions using artificial neural networks. *Ind. Eng. Chem. Res.* **2008**, *47*, 3225–3232.
- (112) Mohammadi, A. H.; Richon, D. Use of artificial neural networks for estimating water content of natural gases. *Ind. Eng. Chem. Res.* **2007**, *46*, 1431–1438.
- (113) Mehrpooya, M.; Mohammadi, A. H.; Richon, D. Extension of an Artificial Neural Network algorithm for estimating sulfur content of sour gases at elevated temperatures and pressures. *Ind. Eng. Chem. Res.* **2010**, *49*, 439–442.
- (114) Gharagheizi, F. A new group contribution-based method for estimation of lower flammability limit of pure compounds. *J. Hazard. Mater.* **2009**, *170*, 595–604.
- (115) Gharagheizi, F. New neural network group contribution model for estimation of lower flammability limit temperature of pure compounds. *Ind. Eng. Chem. Res.* **2009**, *48*, 7406–7416.
- (116) Gharagheizi, F.; Sattari, M. Estimation of molecular diffusivity of pure chemicals in water: A quantitative structure-property relationship study. *SAR & QSAR Environ. Res.* **2009**, *20*, 267–285.
- (117) Gharagheizi, F. Prediction of standard enthalpy of formation of pure compounds using molecular structure. *Aust. J. Chem.* **2009**, *62*, 376–381.
- (118) Gharagheizi, F.; Tirandazi, B.; Barzin, R. Estimation of aniline point temperature of pure hydrocarbons: A Quantitative Structure-Property Relationship approach. *Ind. Eng. Chem. Res.* **2009**, *48*, 1678–1682.
- (119) Gharagheizi, F.; Mehrpooya, M. Prediction of some important physical properties of sulfur compounds using QSPR models. *Mol. Divers.* **2008**, *12*, 143–155.
- (120) Sattari, M.; Gharagheizi, F. Prediction of Molecular Diffusivity of Pure Components into Air: A QSPR Approach. *Chemosphere* **2008**, *72*, 1298–1302.
- (121) Gharagheizi, F.; Alamdari, R. F.; Angaji, M. T. A new neural network-group contribution method for estimation of flash point. *Energ. Fuel.* **2008**, *22*, 1628–1635.
- (122) Gharagheizi, F.; Fazeli, A. Prediction of Watson characterization factor of hydrocarbon compounds from their molecular properties. *QSAR Comb. Sci.* **2008**, *27*, 758–767.
- (123) Gharagheizi, F.; Alamdari, R. F. A molecular-based model for prediction of solubility of c60 fullerene in various solvents. *Fullerenes, Nanotubes, Carbon, Nanostruct.* **2008**, *16*, 40–57.
- (124) Gharagheizi, F. A New neural network quantitative structure-property relationship for prediction of θ (Lower Critical Solution Temperature) of polymer solutions. *e-Polym.* **2007**, *114*, 1–5.
- (125) Gharagheizi, F. QSPR studies for solubility parameter by means of genetic algorithm-based multivariate linear regression and generalized regression neural network. *QSAR Combin. Sci.* **2008**, *27*, 165–170.
- (126) Gharagheizi, F. A chemical structure-based model for estimation of upper flammability limit of pure compounds. *Energ. Fuel.* **2010**, *27*, 3867–3871.
- (127) Vatani, A.; Mehrpooya, M.; Gharagheizi, F. Prediction of standard enthalpy of formation by a QSPR Model. *Int. J. Mol. Sci.* **2007**, *8*, 407–432.
- (128) Mehrpooya, M.; Gharagheizi, F. A Molecular approach for prediction of sulfur compounds solubility parameters, phosphorus sulfur and silicon and related elements. *Phosphorus Sulfur* **2010**, *185*, 204–210.
- (129) Mehta, A. P.; Sloan, E. D. Structure H hydrate phase equilibria of methane + liquid hydrocarbon mixtures. *J. Chem. Eng. Data* **1993**, *38*, 580–582.
- (130) Hütz, U.; Englezos, P.; Measurement of structure H hydrate phase equilibrium and effect of electrolytes. In Proc. 7th International Conference on Fluid Properties and Phase Equilibria for Chemical Process Design, 1995.
- (131) Tohidi, B.; Danesh, A.; Todd, A.; Burgass, R. W.; Østergaard, K. K. Equilibrium data and thermodynamical modelling of cyclopentane and neopentane hydrates. *Fluid Phase Equilib.* **1997**, *138*, 241–250.
- (132) Thomas, M.; Behar, E.; Structure H hydrate equilibria of methane and intermediate hydrocarbon molecules. Proc. 73rd Gas Processors Association Convention, New Orleans, LA, March 7–9, 1995.
- (133) Makogon, T. Y.; Mehta, A. P.; Sloan, E. D. Structure H and structure I hydrate equilibrium data for 2,2-dimethylbutane with methane and xenon. *J. Chem. Eng. Data* **1996**, *41*, 315–318.
- (134) Ohmura, R.; Matsuda, S.; Uchida, T.; Ebinuma, T.; Narita, H. Phase equilibrium for structure-H hydrates at temperatures below the freezing point of water. *J. Chem. Eng. Data* **2005**, *50*, 993–996.
- (135) Mehta, A. P.; Sloan, E. D. Structure H hydrate phase equilibria of paraffins, naphthenes, and olefins with methane. *J. Chem. Eng. Data* **1994**, *39*, 887–890.
- (136) Danesh, A.; Tohidi, B.; Burgass, R. W.; Todd, A. C. Hydrate equilibrium data of methyl cyclopentane with methane or nitrogen. *Trans. IChemE.* **1994**, *72*, 197–200.
- (137) Makino, T.; Nakamura, T.; Sugahara, T.; Ohgaki, K. Thermodynamic stability of structure-H hydrates of methylcyclopentane and cyclooctane helped by methane. *Fluid Phase Equilib.* **2004**, *218*, 235–238.
- (138) Mehta, A. P.; Sloan, E. D. A thermodynamic model for structure-h hydrates. *AIChE J.* **1994**, *40*, 312–320.
- (139) Tohidi, B.; Danesh, A.; Burgass, R.; Todd, A. Hydrate equilibrium data and thermodynamic modelling of methylcyclopentane

and methylcyclohexane in Proc. Second International Conference on Natural Gas Hydrates (Monfort, J. P., ed.), Toulouse, 2–6 June, 109, 1996.

(140) Sloan, E. D. *Clathrate Hydrates of Natural Gases*, 2nd ed.; Marcel Dekker, Inc.: New York, 1998.

(141) Nakamura, T.; Makino, T.; Sugahara, T.; Ohgaki, K. Stability boundaries of gas hydrates helped by methane—structure-H hydrates of methylcyclohexane and cis-1,2-dimethylcyclohexane. *Chem. Eng. Sci.* **2003**, *58*, 269–273.

(142) Mehta, A. P. A Thermodynamic Investigation of Structure H Clathrate Hydrates, Ph.D. Thesis, Colorado School of Mines: Golden, CO, 1996.

(143) Lederhos, J. P.; Mehta, A. P.; Nyberg, G. B.; Warn, K. J.; Sloan, E. D. Structure H clathrate hydrate equilibria of methane and adamantane. *AIChE J.* **1992**, *38*, 1045–1048.

(144) Hara, T.; Hashimoto, S.; Sugahara, T.; Ohgaki, K. Large pressure depression of methane hydrate by adding 1,1-dimethylcyclohexane. *Chem. Eng. Sci.* **2005**, *60*, 3117–3119.

(145) Nakamura, T.; Sugahara, T.; Ohgaki, K. Stability boundary of the structure-H hydrate of cis-1,4-dimethylcyclohexane helped by methane. *J. Chem. Eng. Data* **2004**, *49*, 99–100.

(146) Todeschini, R.; Consonni, V. *Molecular Descriptors for Chemoinformatics*: Vol. I: Alphabetical Listing/Vol. II: Appendices, References, 2nd, Revised and Enlarged ed.. Wiley-VCH: Weinheim, Germany, 2009.

(147) Talete srl, Dragon for Widows (Software for molecular Descriptor Calculation). Version 5.5, 2006.

(148) Milano chemometrics and QSAR research group.

(149) Hyperchem Release 7.5 for Windows, *Molecular Modeling System*; Hypercube, Inc., 2002.

(150) Draper, N.; Smith, H. *Applied Regression Analysis*; John Wiley & Sons, Inc.: New York, 1998.

(151) Holland, J. H. *Adaptation in Natural and Artificial Systems*; University of Michigan Press: Ann Arbor, 1975.

(152) Leardi, R.; Boggia, R.; Terrile, M. Genetic Algorithms as a Strategy for Feature Selection. *J. Chemometr.* **1992**, *6*, 267.

(153) Todeschini, R.; Consonni, V.; Mauri, A.; Pavan, M. Detecting “bad” Regression Models: Multicriteria Fitness Functions in Regression Analysis. *Anal. Chim. Acta* **2004**, *515*, 199.

(154) Suykens, J. A. K.; Van Gestel, T.; De Brabanter, J.; De Moor, B.; Vandewalle, J.; *Least Squares Support Vector Machines*; World Scientific: Singapore, 2002.

(155) Gharagheizi, F. QSPR analysis for intrinsic viscosity of polymer solutions by means of GA-MLR and RBFNN. *Comput. Mater. Sci.* **2007**, *40*, 159.

(156) Gharagheizi, F.; Eslamimanesh, A.; Mohammadi, A. H.; Richon, D. Determination of solubility parameter of non-electrolyte organic compounds: quantitative structure–property relationship strategy. Submitted to *Ind. Eng. Chem. Res.* **2011**.

(157) Liu, H.; Yao, X.; Zhang, R.; Liu, M.; Hu, Z.; Fan, B. Accurate quantitative structure-property relationship model to predict the solubility of C₆₀ in various solvents based on a novel approach using a least-squares support vector machine. *J. Phys. Chem. B* **2005**, *109*, 20565–20571.

(158) Yao, X.; Liu, H.; Zhang, R.; Liu, M.; Hu, Z.; Panaye, A.; Doucet, J. P.; Fan, B. QSAR and classification study of 1,4-dihydropyridine calcium channel antagonists based on least squares support vector machines. *Mol. Pharm.* **2005**, *5*, 348–356.

(159) Manallack, D. T.; Livingstone, D. J. Neural networks in drug discovery; Have they lived up to their promise? *Eur J. Med. Chem.* **1999**, *34*, 195–208.

(160) Gunn, S. R.; Brown, M.; Bossley, K. M. Network performance assessment for neurofuzzy data modeling Lect. *Notes Comput. Sci.* **1997**, *1280*, 313–323.

(161) Suykens, J. A. K.; Vandewalle, J. Least squares support vector machine classifiers. *Neural Process. Lett.* **1999**, *9*, 293–300.

(162) Pelckmans, K.; Suykens, J. A. K.; Van Gestel, T.; De Brabanter, D.; Lukas, L.; Hamers, B.; De Moor, B.; Vandewalle, J. *LS-SVMLab: a Matlab/C Toolbox for Least Squares Support Vector Machines*; Internal Report 02–44, ESATSISTA; K. U. Leuven: Leuven, Belgium, 2002.

(163) Krzanowski, W. J. *Principles of Multivariate Analysis: A User's Perspective*; Oxford University Press: New York, 1988.

(164) Price, K.; Storn, R. Differential Evolution. *Dr. Dobb's J.* **1997**, *22*, 18–24.

(165) Chiou, J. P.; Wang, F. S. Hybrid method of evolutionary algorithms for static and dynamic optimization problems with applications to a fed-batch fermentation process. *Comput. Chem. Eng.* **1999**, *23*, 1277–1291.

(166) Schwefel, H. P. *Numerical Optimization of Computer Models*; John Wiley & Sons: New York, 1981.

(167) Goldberg, D. E. *Genetic Algorithms in Search, Optimization, and Machine Learning*; Addison-Wesley: Reading, MA, 1989.

(168) Davis, L. *Handbook of Genetic Algorithms*; Van Nostrand Reinhold: New York, 1991.

(169) Storn, R. Differential evolution – A simple and efficient heuristic for global optimization over continuous spaces. *J. Global Optim.* **1997**, *11*, 341–359.

(170) Eslamimanesh, A. A semicontinuous thermodynamic model for prediction of asphaltene precipitation in oil reservoirs, M.Sc. Thesis; Shiraz University: Shiraz, Iran, 2009 (In Persian).

(171) Eslamimanesh, A.; Shariati, A. A Semicontinuous thermodynamic model for prediction of asphaltene precipitation, *Presented at VIII Iberoamerican Conference on Phase Equilibria and Fluid Properties for Process Design (Equifase)*, Praia da Rocha, Portugal, Oct. 2009.

(172) Yazdizadeh, M.; Eslamimanesh, A.; Esmailzadeh, F. Thermodynamic modeling of solubilities of various solid compounds in supercritical carbon dioxide: Effects of equations of state and mixing rules. *J. Supercrit. Fluids* **2011**, *55*, 861–875.

(173) Cardoso, M. F.; Salcedo, R. L.; Feyo de Azevedo, S.; Barbosa, D. A simulated annealing approach to the solution of minlp problems. *Comput. Chem. Eng.* **1997**, *21*, 1349–1364.

(174) Hagan, M.; Demuth, H. B.; Beale, M. H. *Neural Network Design*; International Thomson Publishing: Boston, 2002.

(175) Eslamimanesh, A.; Yazdizadeh, M.; Mohammadi, A. H.; Richon, D. Experimental data assessment test for diamondoids solubility in gaseous system. *J. Chem. Eng. Data* **2011**, *56*, 2655–2659.

(176) Eslamimanesh, A.; Mohammadi, A. H.; Richon, D. Thermodynamic consistency test for experimental data of water content of methane. *AIChE J.* **2011** In press, DOI: 10.1002/aic.12462.

(177) Coquelet, C.; Galicia-Luna, L. A.; Mohammadi, A. H.; Richon, D. The essential importance of experimental research and the use of experimental thermodynamics to the benefit of industry. *Fluid Phase Equilib.* **2010**, *296*, 2–3.